Received Date : 18-Jul-2016
Revised Date : 12-Oct-2016
Accepted Date : 25-Oct-2016
Article type : Research Article

Synthesis, cytotoxic activity, 2D- and 3D-QSAR studies of 19-carboxyl modified novel isosteviol derivatives as potential anticancer agents

Cong-Jun Liu [a], Tao Zhang [b], Shu-Ling Yu [c], Xing-Jie Dai [a], Ya Wu [a], Jing-Chao Tao* [a]

[a] College of Chemistry and Molecular Engineering, New Drug Research & Development Center, Zhengzhou University, 75 Daxue Road, Zhengzhou, Henan 450052, China

[b] School of Pharmacy, Xinxiang Medical University, Xinxiang 453003, Henan, China

[c] Key Laboratory of Natural Medicine and Immune-Engineering of Henan Province, Henan University, Kaifeng, Henan 475004, China

Abstract: Two series of novel acylthiosemicarbazide and oxadiazole fused-isosteviol derivatives were synthesized based on the 19-carboxyl modification. The target compounds were evaluated for their cytotoxicities against 3 cancer cell lines (HCT-116, HGC-27 and JEKO-1) using an MTT assay. Lead compounds from the acylthiosemicarbazides (**4**) showed IC_{50} values in the lower μmolar range. For example, compounds (**4i**, **4l**, **4m**, **4r** and **4s**) exhibited significant inhibitory activities against the 3 cell lines with IC_{50} values of 0.95-3.36 μM. Furthermore, 2D-HQSAR and 3D-topomer CoMFA analyses were established, which could be used to develop second generation of isosteviol derivatives as anticancer agents.

Key words: Isosteviol derivatives; Synthesis; Cytotoxicity; 2D-HQSAR; 3D-topomer CoMFA.

* Corresponding author. Tel/Fax: +86-371-67767200. Email address: jctao@zzu.edu.cn.

1. Introduction

Cancer, the second leading cause of death after cardiovascular disorders, represents one of the most serious clinical problems and its incidence is rapidly rising throughout the world (1-3). Despite recent advances in cancer therapy, numerous anticancer drugs have been reported which are having severe side effects. Development of novel compounds as chemotherapeutic agents having a limited toxicity profile is needed. Natural products and their derivatives, such as doxorubicin, paclitaxel, vinblastine, are a rich source of treatments for cancers, and the unique metabolites produced by diterpenoids have increasingly become major players in anticancer drug discovery (4-8).

Isosteviol (*ent*-16-oxobeyeran-19-oic acid), a metabolite of stevioside isolated from the leaves of the natural *stevia* plant, is a tetracyclic diterpenoid with a beyerane skeleton which becomes one of the most popular platforms for the design of novel pharmacological agents (9, 10). Previous studies have found that isosteviol exhibits a wide range of biological activities, including antihypertension (11, 12), antihyperglycemic (13, 14), antioxidative (15), antidiarrheal (16), cardio- and neuroprotective effects (17, 18). To go deep into the research on isosteviol, a large number of isosteviol derivatives have been obtained by microbial transformation and chemical modification. The typical properties of isosteviol derivatives, such as cytotoxic activities (19-23), catalytic performance (24-27), as well as supramolecular self-assembly properties (28-30), were further investigated in recent years. Notably, some of the synthetic isosteviol derivatives exhibited remarkable inhibitory activity against cancer cells that captured scientific attention with possible applications in anticancer drugs design and development. Indeed, recently published novel cytotoxic isosteviol derivatives with D-ring modifications have shown promising results. Notable example is the exo-methylene cyclopentanone tetracyclic diterpenoids **A**, which exhibited similar anticancer activities to adriamycin with IC_{50} value of 1.58 μM (31). Moreover, some bioactive subunits containing isosteviol derivatives, such as 1,3-amino alcohol fragment **B** (32) or triazole ring **C** (33), were proved to possess antiproliferative activities on several human malignant cell lines. And the heterocycle bridged carbothioamide type isosteviol derivatives **D**, **E** (34) showed remarkable cytotoxic activities (Fig. 1). However, few reports have been focused on introduction of bioactive structural fragments to 19-position of isosteviol. In addition, to the best of our knowledge, two-dimensional hologram quantitative structure–activity relationship (2D-HQSAR) and three-dimensional topomer comparative molecular field analyses (3D-topomer CoMFA) were scarcely employed to investigate the structure–activity relationship

of 19-carboxyl modified isosteviol derivatives.

In light of these facts, two series of novel isosteviol derivatives containing acylthiosemicarbazide and oxadiazole moieties based on 19-carboxyl modification were synthesized in the present work, and their cytotoxicities against HCT-116, HGC-27 and JEKO-1 cancer cell lines *in vitro* were evaluated. Furthermore, two- and three-dimensional quantitative structure–activity relationships were also studied for the validation of the observed pharmacological properties of the investigated bioactive compounds and for the confirmation of the most important parameters controlling these properties. The contribution/contour maps, displaying activity information, will be further taken advantage of designing new anticancer molecules with improved potency.

2. Results and discussion

2.1. Chemistry

Synthesis of isosteviol-fused acylthiosemicarbazide subunit or oxadiazole ring was carried out as the route shown in Scheme 1. The initial isosteviol **1** was obtained through the sulfuric acid hydrolysis of stevioside. Its acid chloride **2** was prepared from compound **1** and oxalyl chloride by adding drops of DMF as catalyst, which then reacted without purification with hydrazine in dichloromethane at -10 ^{o}C to furnish compound **3** in 89% yield. Compounds **4a-4u,** the acylthiosemicarbazide subunit containing isosteviol derivatives, were readily synthesized through condensation of compound **3** with appropriately substituted phenyl isothiocyanates in dichloromethane with the final yields of 37–89%. The IR spectrum of compound **4s**, as a representative example of the synthesized compounds, shows absorption bands of N-H group at 3312 cm^{-1} and of C=O, C=S moieties at 1735, 1330 cm^{-1}, respectively. In its NMR spectra, resonances are distinctly observed at δ_H 10.54, 9.61, 9.19 ppm and δ_C 178.86, 171.27ppm, demonstrating the formation of acylthiosemicarbazide substructure. Subsequently, cyclization of compounds **4a-4u** took place readily in refluxing ethanol in the presence of mercuric acetate to afford the corresponding oxadiazole derivatives **5a-5u**.

In order to further investigate the effects of thiourea subunit and carbonyl group on anticancer activities, and simultaneously to provide diverse molecule structures convenient for the subsequent QSAR studies, compounds **6**, **7** and **8** were also designed and synthesized. The synthetic approaches employed to prepare the target derivatives were outlined in Scheme 2**.** Treatment of compound **3** with phenyl isocyanate afforded the corresponding target compound **6** in good yield. Meantime, the C(16)=O group of compound

5a was reduced with sodium borohydride to give the compound **7**, which was further acylated with acetic anhydride in pyridine at room temperature to generate the compound **8** with the yield of 97%.

2.2. Evaluation of cytotoxic activity

The *in vitro* cytotoxic activity of the novel isosteviol derivatives obtained was examined in three human cancer cell lines: colon carcinoma (HCT-116), gastric carcinoma (HGC-27), mantle cell lymphoma (JEKO-1) using the MTT assay. Cisplatin was included in the experiments as a positive control. The IC_{50} values were summarized in Table 1.

From the obtained results we can see that all the investigated isosteviol derivatives exhibited much better cytotoxic activities than their precursor isosteviol **1**. Acylthiosemicarbazides-substituted isosteviol derivatives **4a**-**4u** displayed much higher cytotoxicities against 3 cancer cell lines than those of the oxadiazoles **5a**-**5u**. Investigations of the cytotoxic activity against HCT-116 demonstrated that it was the most sensitive cell line to the influence of the tested compounds.

The inhibitory activities against HCT-116 and HGC-27 cell lines were remarkablely improved as the introduction of the substituted acylthiosemicarbazides to the isosteviol skeleton (**4a-4u** vs **3**). Notably, compounds (**4i**, **4l**, **4m**, **4r** and **4s**) exhibited IC_{50} values in the lower μmolar range (0.95-3.36 μM). Going even further, substituted groups and positions on aromatic ring had a significant effect on cytotoxic activities. Compounds with strong electron-withdrawing substituents (**4e-4g, 4r** and **4s**) exhibited good to excellent cytotoxic activities. Except for the compounds (**4q-4s**), the *meta*-substituted compounds were more favorable to the cytotoxicity than the *ortho* and *para*-substituted compounds. However, replacement of the sulfur with oxygen greatly decreased the cytotoxic activities (**4a** vs **6**), which indicated that the thiocarbamide moiety may play an important role in the influence to cytotoxic activity. What's more, most of cyclized oxadiazole compounds revealed the moderate cytotoxic activity. Only compound **5g** showed better inhibitory activity against JEKO-1 cells than the positive control cisplatin. But to our disappointment, when the carbonyl group was reduced to hydroxyl or further acylated, the compounds (**7**, **8**) showed poor inhibitory activities against JEKO-1 cell with IC_{50} values of 57.24±2.5 μM and 52.53±2.4 μM, respectively. In order to further understand the observed cytotoxic activities and determine the main controlling factors governing these activities, quantitative structure–activity relationship (QSAR) studies were developed.

2.3. QSAR studies

2.3.1. Data sets

Forty six isosteviol derivatives (**3**-**8**) were used for the QSAR analyses, of which thirty seven compounds were selected as training set to construct model and the other nine (**4a**, **4b**, **4j**, **4r**, **4u**, **5e**, **5l**, **5p**, **7**) were assigned into test set for external model validation. The division of the dataset was done randomly, but taking into account the diversity of the bioactivities simutaneously. The IC_{50} values against HCT-116 cells, which was the most sensitive to the influence of the tested compounds, were converted into the corresponding pIC_{50} ($-\log IC_{50}$) and subsequently used as dependent variables for the 2D-HQSAR and 3D-topomer CoMFA analyses.

2.3.2. 2D- and 3D-QSAR model development

Three distinct parameters, such as hologram length, fragment distinction and fragment size, were used to generate the 2D-HQSAR model. For the hologram length, default values of 53, 59, 61, 71, 83, 97, 151, 199, 257, 307, 353 and 401 were implemented in SYBYL. The fragment distinction for displaying molecule information was described in terms of atoms (A), bonds (B), connections (C), hydrogen (H), chirality (Ch), donor and acceptor (DA). The minimum (*M*) and maximum (*N*) number of atoms of the broken molecule was defined as fragment size which was provided as default value of 4–7. Three distinct parameters as independent variables were linearly correlated with the pIC_{50} values as dependent variables by the full cross validated (q^2) partial least square (PLS) leave-one-out (LOO) method to develop the 2D-HQSAR model.

Initially, the influence of the fragment distinction parameters on the statistical values of models was investigated. A series of 2D-HQSAR models (Table 2) were developed by the combination of more than one fragment distinction parameters, while fragment size (4–7) and hologram length (53 to 401) were respectively set. As shown in Table 2, q^2 value of 2D-HQSAR model based on the combination of A and B (model 1) is 0.413. An introduction of the factor H into the combination of A and B could improve the q^2 value (model 3, q^2 = 0.498), whereas the introduction of factor C resulted in the decreasing of q^2 value (model 2, q^2 = 0.368), indicating that connections (C) did not represent their intrinsic structural characteristics. Introducing Ch or DA into the combination of A/B/H, respectively, could further improve the q^2 value. Especially, the combination of A/B/H/DA could generate the highest q^2 value of 0.589 (model 9). However, simultaneously introduction of Ch and DA into the combination of A/B/H could not further increase the q^2 value (q^2 = 0.577). Therefore, the A/B/H/DA combination was proved to be the most

effective fragment distinction.

Based on the best 2D-HQSAR model (model 9, Table 2), the influences of distinct fragment sizes on the statistical parameters were further investigated. The statistical results, summarized in Table 3, demonstrated that the variation of fragment size led to the generation of a better 2D-HQSAR model on the basis of the fragment size of 7–8, affording the highest q^2 value of 0.631 (model 13). Therefore, the final optimal 2D-HQSAR model, demonstrating the q^2, SEcv, r^2 and SEE values of 0.631, 0.249, 0.882 and 0.140, respectively, was developed by using A/B/H/DA as fragment distinction parameters, 7–8 as fragment size, and 6 as optimum number of component.

In the 3D-topomer CoMFA analysis, C-4 and C-19 were initially picked respectively from the two most active compounds of their respective series, **4s** and **5f**，which were taken as the two template molecules. All the training set compounds were automatically divided into R_1 (blue) and R_2 (red) fragments (Fig. 2). Two fragments were applied with topomer alignment to make a 3D invariant representation. Steric and electrostatic interaction energies were calculated using carbon sp^3 probe. These steric and electrostatic field descriptor values and the cytotoxicities as independent and dependent variables, respectively, were correlated to finally generate the 3D-topomer CoMFA model, which provided a cross-validated q^2 value of 0.572, an optimized component of 3, and a noncross-validated r^2 value of 0.853 with cross-validated standard error SE_{CV} = 0.25 and noncross validated standard error SEE = 0.15. These data demonstrate that the model has a predictive ability of (q^2 >0.2).

2.3.3. Validation of the 2D- and 3D-QSAR models

The statistical parameters of the optimal models selected by the 2D- and 3D-QSAR methods were summarized in Table 4. In order to investigate the predictive ability of the constructed QSAR models based on the training set, an external test set including nine compounds was used for validation. The cytotoxicities against HCT-116 cells of the 9 test set compounds were predicted using the two optimal models. The 2D-HQSAR and 3D-topomer CoMFA models afforded the satisfactory r^2_{pred} values of 0.832 and 0.643 (Table 4), respectively. Comparing with the r^2_{pred} value of 3D-topomer CoMFA model, the 2D-HQSAR model had the better predictive r^2 value and showed good predictions for the external test set, indicating that the 2D-HQSAR method are more suited to this kind of datasets than 3D-topomer CoMFA method.

The detailed experimental and predicted cytotoxicities (pIC_{50}) with residual values for the test set compounds from the two models were listed in Table 5. The predicted pIC_{50} residuals of 2D-HQSAR and 3D-topomer CoMFA models were less than 0.3 and 0.4 log unit, respectively, indicating that high predictive QSAR models were obtained. The histogram of residual values (Fig. 3) visually displayed that the 2D-HQSAR model had smaller residuals than 3D-topomer CoMFA model.

The correlation between the experimental and predicted activities of both the training set and the test set was also displayed graphically in Fig. 4. It was shown that the predicted values of all compounds fall closely to the experimental pIC_{50} values almost in a line, deviating by no more than 0.3 log units except compounds **4b**, **4u** and **5t**. The good agreement between experimental and predicted pIC_{50} values for the training set and test set compounds indicates the internal robustness and external high prediction of the QSAR models.

2.3.4. Atomic contribution maps and contour maps analyses

A significant role of QSAR model, besides predicting the activities of untested molecules, is to provide straightforward clues about the relationship between molecular fragments and bioactivities (35). In 2D-HQSAR analysis, the results can be graphically displayed in the form of contribution maps, where the color coding of each atom reflects its contribution to the overall activity of the molecule. The color (red, red orange and orange) at one end of the spectrum denotes the negative contribution (NC) to the activity, whereas the color (yellow, green blue and green) of the other end reflects positive contribution (PC) to the activity. Additionally, the intermediate contribution (IC) is indicated by white color.

The individual atomic contribution maps of compounds **4s**, **4u**, **5f** and **5t,** the highest and the lowest active compounds in their respective series, were depicted in Fig. 5. It can be seen from the map, the 4'-nitrophenyl, ring A and ring B of compound **4s** are colored yellow and green, respectively, indicating favorable contribution to the cytotoxic activity. The 2, 6-dimethylphenyl group was heavily colored red in compound **4u** showing significant negative effect on bioactivity. Moreover, ring A and ring B of compound **4u** was colored white and red orange, demonstrating their intermediate or negative contribution to the cytotoxic activity. In the representations of compounds **5f** and **5t**, the particular atoms in the oxadiazole ring were colored yellow, suggesting that the heterocycle subunit may be the pharmacologically important group. In addition, the facts that there are more yellow areas and less red areas in compound **5f** than in compound **5t** can reasonably explain the more potent cytotoxicity of compound **5f**. Furthermore, in any molecule of the dataset, regions with intermediate or unfavorable contributions can be identified as the

potential targets for the structural modification as well as the SAR studies.

In the 3D-topomer CoMFA analysis, the contour maps around R_1 and R_2 (Fig. 6) were obtained by plotting the coefficients from the 3D-topomer CoMFA model. The most active compound **4s** was chosen as a reference structure to explain the contour map. In the steric contour map, green color represents that sterically bulky group is in favor of activity, whereas yellow color is unfavoured for activity. In the electrostatics contour map, red and blue colors denote respectively electronegative or electropositive groups favored for activity.

As shown in Fig. 6, a yellow region (Fig. 6, A) near the C-16 of the R_1 fragment indicates that the bulk groups are unfavorable to the anticancer activity. This can well explain the fact that compound **8** containing large group at this position has relative lower anticancer activity (IC_{50} = 15.06±1.3 μM) than compound **5a** (IC_{50} = 9.56±0.9 μM). The skeleton of R_1 fragment lacks of distinct substituent so that the electrostatics contour maps are not found around it (Fig. 6, B). In Fig. 6 (C), a green contour near the *meta*- and *para*-position of the phenyl group in R_2 fragment suggests that a bulky group would be in favor of activities (e.g. compound **4l** having *meta*-Br group with IC_{50} = 1.35±0.3 μM, whereas compound **4i** having *meta*-Cl group with IC_{50} = 1.62±0.1 μM). While the yellow contour near *ortho*-position of the phenyl group, unfavoured result was observed (compound **4b** having *ortho*-CH_3 group with IC_{50} = 11.61±0.9 μM). Furthermore, a large red region surrounding *para*-position of the phenyl group (Fig. 6, D) demonstrates that introduction of electronegative groups can improve the inhibitory activity (e.g. compound **4g** having *para*-F group with IC_{50} = 2.40±0.5 μM, whereas compound **4s** having *para*-NO_2 group with IC_{50} = 0.95±0.1 μM). Based on the above useful clues and informations from atomic contribution and contour maps analyses, a conclusion can be derived that the introduction of small group(s) onto the C-16 position of the isosteviol fragment and electron-withdrawing and bulky group(s) onto the *para*-position of the phenyl group may be favorable for the inhibitory activity against HCT-116 cells.

3. Conclusions

In this work, two series of 19-carboxyl modified novel isosteviol derivatives, containing respectively acylthiosemicarbazide and oxadiazole subunits, were rationally designed and successfully synthesized. Their cytotoxic activities *in vitro* against three human cancer cell lines (HCT-116, HGC-27 and JEKO-1) were evaluated. The results obtained revealed that the HCT-116 cell line was more sensitive to the novel compounds than the HGC-27 and JEKO-1 cell lines. It was noteworthy that the acylthiosemicarbazide

group containing isosteviol derivatives exhibited prominent cytotoxicities against all the three cell lines. Especially, compounds (**4i**, **4l**, **4m**, **4r** and **4s**) exhibited the significant inhibitory activities against the 3 cell lines with IC_{50} values of 0.95-3.36 μM, which may be exploitable as lead compounds for the development of potent antitumor agents. In addition, 2D- and 3D-QSAR techniques were implemented on the SAR of these compounds. The optimal 2D-HQSAR and 3D-topomer CoMFA models with good predictive capabilities were obtained. Based on the useful clues and informations from atomic contribution maps and contour maps generated by 2D-HQSAR and 3D-topomer CoMFA models, a conclusion can be derived that introduction of small group(s) onto the C-16 position of isosteviol and electron-withdrawing and bulky group(s) onto the *para*-position of the phenyl group may be favorable for the inhibitory activity against HCT-116 cells. The results provided a practical method for the development of second generation of isosteviol derivatives as anticancer agents.

4. Experimental protocols

4.1. General procedures

All chemicals were used as received unless otherwise noted. Reagent grade solvents were redistilled prior to use. Isosteviol **1** was synthesized as described by Wu et al (36). Chromatography was performed on silica gel (100-200 mesh). All melting points were measured with a Beijing Keyi XT5 apparatus and the temperature was not corrected. The IR spectra were recorded as KBr pellets on a Thermo Nicolet (IR200) spectrometer. ^{1}H and ^{13}C NMR spectra were collected with a Bruker DPX-400 spectrometer at 400 and 100 MHz, respectively, with TMS as internal standard. High-resolution mass spectra (HRMS) were obtained with a Waters Micromass Q-Tof Micro™ instrument by the ESI technique. X-ray analysis was taken on a Rigaku Saturn 724 CCD diffractomer (Mo-Kα, λ = 0.71073 Å).

4.2. The preparation of isosteviol derivatives

4.2.1. Compound 2

To a solution of compound **1** (0.318 g, 1 mmol) in CH_2Cl_2 (10 mL), oxalyl chloride (0.191 g, 1.5 mmol) was added and the resulting mixture was stirred for 30 min. To this was added the DMF (0.1 ml) and stirring was continued at room temperature for 8 h. Upon completion, the solvent was evaporated in vacuo to obtain the crude product **2** as a gray solid, which was used directly in the next step without further purification.

4.2.2. Compound 3

The crude product **2** (0.366 g, 1 mmol) was dissolved in CH_2Cl_2 (20 mL) at -10 ^oC, and then 80% hydrazine hydrate (0.1 mL, 2 mmol) was slowly added. After stirring for 2 h, the mixture was washed with saturated NaCl aqueous solution, dried with anhydrous sodium sulfate, filtered and concentrated under vacuum. The residue was purified by column chromatography on silica (dichloromethane / methanol = 5:1, v/v) to give the compound **3** as a white powder. Yield 89%; Mp 82.3–84.1 °C; IR (KBr): 3323, 2925, 2846, 1737, 1633, 1503, 1454, 1402, 1372, 1321, 1249, 1199, 1151, 1110, 1087, 1028, 977, 916, 734, 695, 590, 508cm^{-1}; ^1H NMR (400MHz, $CDCl_3$, ppm): δ 7.02 (s, 1H), 3.48 (s, 2H), 2.63 (d, J = 18.64Hz, 1H), 2.03 (d, J = 14.32Hz, 1H), 1.95 (d, J = 13.52Hz, 1H), 1.83–1.67 (m, 6H), 1.62–1.48 (m, 4H), 1.42–1.33 (m, 2H), 1.27–1.21 (m, 1H), 1.19 (s, 3H), 1.15–1.03 (m, 2H), 0.97 (s, 3H), 0.94–0.79 (m, 2H), 0.74 (s, 3H); ^{13}C NMR (100MHz, $CDCl_3$, ppm): δ 222.11, 177.52, 57.56, 54.67, 54.22, 48.68, 48.37, 43.04, 41.56, 40.00, 39.44, 38.01, 37.44, 37.24, 29.99, 22.11, 20.31, 19.83, 19.11, 13.44; HRMS (ESI, *m/z*) calcd for $C_{20}H_{33}N_2O_2$ $[M+H]^+$ 333.2542. Found: 333.2539.

4.2.3. General procedure for synthesis of compounds 4a-4u

Compound **3** (0.332 g, 1 mmol) was dissolved in CH_2Cl_2 (10 mL). Appropriately substituted phenyl isothiocyanates (1.1 mmol) was added. The reaction mixture was stirred at room temperature. After completion of the reaction monitored by TLC, the solvent was removed under reduced pressure. The residue was purified by column chromatography on silica to give the target compound **4a-4u**.

*4.2.3.1. Compound **4a***. White powder; Yield 64%; Mp 87.5–88.4 °C; IR (KBr): 3300, 3056, 2928, 2847, 1734, 1653, 1598, 1534, 1497, 1447, 1353, 1319, 1235, 1155, 1110, 1088, 1032, 973, 900, 854, 694, 590, 499 cm^{-1}; ^1H NMR (400MHz, $CDCl_3$, ppm): δ 10.08 (s, 1H), 9.83 (s, 1H), 8.68 (s, 1H), 7.43–7.26 (m, 5H), 2.59 (d, J = 18.44Hz, 1H), 2.16 (d, J = 14.24Hz, 1H), 1.99–1.87 (m, 3H), 1.80–1.67 (m, 4H), 1.62–1.50 (m, 5H), 1.44–1.33 (m, 3H), 1.28 (s, 3H), 1.27–1.18 (m, 2H), 0.97 (s, 3H), 0.92–0.89 (m, 1H), 0.79 (s, 3H); ^{13}C NMR (100MHz, $CDCl_3$, ppm): δ 222.10, 176.22, 172.05, 136.99, 129.46, 129.46, 126.91, 125.30, 125.30, 57.51, 54.58, 54.09, 48.67, 48.24, 43.11, 41.31, 39.87, 39.37, 38.08, 37.23, 37.18, 30.18, 22.20, 20.31, 19.81, 18.89, 13.75; HRMS (ESI, *m/z*) calcd for $C_{27}H_{38}N_3O_2S$ $[M+H]^+$ 468.2685. Found: 468.2683.

*4.2.3.2. Compound **4b***. White powder. Yield 60%; Mp 112.1–114.9 °C; IR (KBr): 3284, 3058, 2929, 2847, 1736, 1643, 1590, 1527, 1458, 1370, 1344, 1246, 1154, 1109, 1045, 973, 855, 728, 698, 632, 510cm^{-1}; ^1H NMR (400MHz, $CDCl_3$, ppm): δ 10.36 (s, 1H), 9.85 (s, 1H), 8.53 (s, 1H), 7.30–7.24 (m, 4H), 2.55 (dd, J = 18.60, 3.48Hz, 1H), 2.31 (s, 3H), 2.11 (d, J = 14.60Hz, 1H), 1.98–1.45 (m, 11H), 1.36–1.30 (m, 4H), 1.25

(s, 3H), 1.21–1.12 (m, 2H), 0.95 (s, 3H), 0.92–0.88 (m, 1H), 0.77 (s, 3H); ^{13}C NMR (100MHz, $CDCl_3$, ppm): δ 222.13, 176.61, 171.48, 135.74, 135.26, 131.28, 128.33, 127.88, 127.15, 57.50, 54.50, 54.04, 48.63, 48.18, 42.97, 41.22, 39.84, 39.29, 38.00, 37.14, 37.06, 30.16, 22.14, 20.27, 19.78, 18.82, 17.91, 13.69; HRMS (ESI, *m/z*) calcd for $C_{28}H_{40}N_3O_2S$ $[M+H]^+$ 482.2841. Found: 482.2839.

4.2.3.3. Compound ***4c***. White powder. Yield 37%; Mp 104.6–107.2 °C; IR (KBr): 3296, 3046, 2927, 2847, 1735, 1652, 1611, 1537, 1451, 1348, 1298, 1249, 1152, 1043, 975, 900, 781, 718, 693, 623, 571cm^{-1}; ^{1}H NMR (400MHz, $CDCl_3$, ppm): δ 9.94 (s, 1H), 9.78 (s, 1H), 8.48 (s, 1H), 7.28 (t, *J* = 7.98Hz, 1H), 7.15 (d, *J* = 9.00Hz, 2H), 7.08 (d, *J* = 7.52Hz, 1H), 2.57 (dd, *J* = 18.60, 3.56Hz, 1H), 2.36 (s, 3H), 2.14 (d, *J* = 14.48Hz, 1H), 1.97–1.31 (m, 14H), 1.25 (s, 3H), 1.24–1.17 (m, 3H), 0.96 (s, 3H), 0.93–0.87 (m, 1H), 0.77 (s, 3H); ^{13}C NMR (100MHz, $CDCl_3$, ppm): δ 222.14, 175.97, 171.89, 139.60, 136.62, 129.34, 127.88, 125.91, 122.31, 57.48, 54.57, 54.09, 48.66, 48.23, 43.05, 41.33, 39.86, 39.35, 38.05, 37.20, 37.16, 30.15, 22.15, 21.39, 20.29, 19.80, 18.89, 13.71; HRMS (ESI, *m/z*) calcd for $C_{28}H_{40}N_3O_2S$ $[M+H]^+$ 482.2841. Found: 482.2840.

4.2.3.4. Compound ***4d***. White powder. Yield 41%; Mp 102.3–104.7 °C; IR (KBr): 3293, 3029, 2926, 2847, 1735, 1652, 1606, 1517, 1449, 1344, 1290, 1236, 1153, 1111, 1044, 974, 818, 727, 694, 586, 500cm^{-1}; ^{1}H NMR (400MHz, $CDCl_3$, ppm): δ 9.94 (s, 1H), 9.80 (s, 1H), 8.59 (s, 1H), 7.22 (d, *J* = 8.56Hz, 2H), 7.19 (d, *J* = 8.48Hz, 2H), 2.58 (dd, *J* = 18.64, 3.48Hz, 1H), 2.34 (s, 3H), 2.13 (d, *J* = 14.44Hz, 1H), 1.96–1.31 (m, 15H), 1.25 (s, 3H), 1.24–1.14 (m, 2H), 0.96 (s, 3H), 0.92–0.89 (m, 1H), 0.77 (s, 3H); ^{13}C NMR (100MHz, $CDCl_3$, ppm): δ 222.15, 176.21, 171.84, 137.02, 134.12, 130.12, 130.12, 125.43, 125.43, 57.48, 54.56, 54.08, 48.65, 48.23, 43.03, 41.33, 39.85, 39.35, 38.04, 37.18, 37.16, 30.15, 22.12, 21.08, 20.29, 19.80, 18.87, 13.71; HRMS (ESI, *m/z*) calcd for $C_{28}H_{40}N_3O_2S$ $[M+H]^+$ 482.2841. Found: 482.2839.

4.2.3.5. Compound ***4e***. White powder. Yield 73%; Mp 102.1–102.3 °C; IR (KBr): 3290, 3041, 2928, 2847, 1734, 1656, 1621, 1542, 1494, 1456, 1342, 1249, 1152, 1107, 1033, 974, 856, 807, 752, 699, 622, 570cm^{-1}; ^{1}H NMR (400MHz, $CDCl_3$, ppm): δ 10.59 (s, 1H), 10.00 (s, 1H), 8.69 (d, *J* = 14.84Hz, 1H),, 7.67 (t, *J* = 7.22Hz, 1H), 7.26–7.13 (m, 3H), 2.56 (dd, *J* = 18.64, 3.12Hz, 1H), 2.13 (d, *J* = 14.76Hz, 1H), 2.00–1.31 (m, 14H), 1.28 (s, 3H), 1.25–1.12 (m, 3H), 0.95 (s, 3H), 0.93–0.87 (m, 1H), 0.79 (s, 3H); ^{13}C NMR (100MHz, $CDCl_3$, ppm): δ 222.08, 176.61, 171.62, 156.66 (d, *J* = 246.06Hz), 128.40 (d, *J* = 2.75Hz), 128.21 (d, *J* = 7.67Hz), 125.50 (d, *J* = 16.44Hz), 124.38, 116.17 (d, *J* = 19.94Hz), 57.52, 54.56, 54.04, 48.67, 48.16, 43.08, 41.26, 39.86, 39.30, 38.06, 37.23, 37.16, 30.14, 22.08, 20.31, 19.80, 18.77, 13.72; HRMS (ESI, *m/z*) calcd for $C_{27}H_{37}FN_3O_2S$ $[M+H]^+$ 486.2591. Found: 486.2588.

4.2.3.6. Compound ***4f***. White powder. Yield 80%; Mp 119.3–121.5 °C; IR (KBr): 3299, 3079, 2928, 2847, 1734, 1655, 1611, 1543, 1490, 1444, 1349, 1283, 1253, 1148, 1045, 970, 861, 776, 721, 682, 571, 519cm^{-1}; ^{1}H NMR (400MHz, $CDCl_3$, ppm): δ 10.47 (s, 1H), 9.89 (s, 1H), 8.88 (s, 1H), 7.33 (q, *J* = 7.54Hz, 1H), 7.25 (d, *J* = 10.00Hz, 1H), 7.16 (d, *J* = 8.00Hz, 1H), 6.94 (td, *J* = 8.16, 1.76Hz, 1H), 2.58 (dd, *J* = 18.60, 3.20Hz, 1H), 2.15 (d, *J* = 14.64Hz, 1H), 1.99–1.32 (m, 14H), 1.27 (s, 3H), 1.25–1.19 (m, 3H), 0.96 (s, 3H), 0.92–0.86 (m, 1H), 0.78 (s, 3H); ^{13}C NMR (100MHz, $CDCl_3$, ppm): δ 222.08, 176.30, 172.25, 162.71 (d, *J* = 245.24Hz), 139.05 (d, *J* = 10.15Hz), 130.20 (d, *J* = 9.28Hz), 120.53, 113.30 (d, *J* = 21.10Hz), 112.44 (d, *J* = 24.04Hz), 57.43, 54.53, 54.01, 48.66, 48.20, 43.13, 41.23, 39.80, 39.35, 38.07, 37.23, 37.13, 30.19, 22.24, 20.29, 19.78, 18.84, 13.70; HRMS (ESI, *m/z*) calcd for $C_{27}H_{37}FN_3O_2S$ $[M+H]^+$ 486.2591. Found: 486.2587.

4.2.3.7. Compound ***4g***. White powder. Yield 89%; Mp 112.5–115.1 °C; IR (KBr): 3294, 3062, 2929, 2847, 1734, 1654, 1509, 1465, 1343, 1220, 1153, 1046, 974, 835, 798, 731, 586, 507cm^{-1}; ^{1}H NMR (400MHz, $CDCl_3$, ppm): δ 10.38 (s, 1H), 9.93 (s, 1H), 8.77 (s, 1H), 7.35–7.31 (m, 2H), 7.10–7.06 (m, 2H), 2.58 (dd, *J* = 18.56, 3.52Hz, 1H), 2.12 (d, *J* = 15.12Hz, 1H), 1.99–1.32 (m, 14H), 1.27 (s, 3H), 1.24–1.17 (m, 3H), 0.96 (s, 3H), 0.94–0.87 (m, 1H), 0.78 (s, 3H); ^{13}C NMR (100MHz, $CDCl_3$, ppm): δ 222.00, 176.87, 171.78, 161.12 (d, *J* = 245.39Hz), 133.28, 127.85 (d, *J* = 7.41Hz), 127.85 (d, *J* = 7.41Hz), 116.11 (d, *J* = 22.64Hz), 116.11 (d, *J* = 22.64Hz), 57.42, 54.51, 54.00, 48.66, 48.22, 43.04, 41.25, 39.80, 39.34, 38.05, 37.19, 37.13, 30.20, 22.24, 20.29, 19.77, 18.81, 13.71; HRMS (ESI, *m/z*) calcd for $C_{27}H_{37}FN_3O_2S$ $[M+H]^+$ 486.2591. Found: 486.2586.

4.2.3.8. Compound ***4h***. White powder. Yield 74%; Mp 114.3–117.1 °C; IR (KBr): 3311, 3062, 2927, 2847, 1735, 1657, 1593, 1537, 1470, 1443, 1340, 1229, 1155, 1129, 1055, 1034, 974, 856, 755, 732, 684, 621, 572, 452 cm^{-1}; ^{1}H NMR (400MHz, $CDCl_3$, ppm): δ 10.57 (s, 1H), 9.99 (s, 1H), 8.78 (s, 1H), 7.67 (d, *J* = 7.24Hz, 1H), 7.47 (dd, *J* = 7.96, 1.36Hz, 1H), 7.33 (td, *J* = 7.66, 1.36Hz, 1H), 7.24 (td, *J* = 7.68, 1.44Hz, 1H), 2.55 (dd, *J* = 18.64, 3.48Hz, 1H), 2.13 (d, *J* = 14.84Hz, 1H), 2.01–1.30 (m, 13H), 1.28 (s, 3H), 1.25–1.11 (m, 4H), 0.95 (s, 3H), 0.93–0.86 (m, 1H), 0.78 (s, 3H); ^{13}C NMR (100MHz, $CDCl_3$, ppm): δ 222.09, 176.59, 171.63, 134.83, 130.64, 130.00, 128.97, 128.19, 127.45, 57.54, 54.51, 54.01, 48.64, 48.16, 43.09, 41.18, 39.83, 39.26, 38.03, 37.12, 30.17, 29.68, 22.15, 20.28, 19.77, 18.77, 13.73; HRMS (ESI, *m/z*) calcd for $C_{27}H_{37}ClN_3O_2S$ $[M+H]^+$ 502.2295. Found: 502.2291.

4.2.3.9. Compound ***4i***. White powder. Yield 80%; Mp 114.0–115.5 °C; IR (KBr): 3294, 3070, 2927, 2848, 1735, 1655, 1594, 1537, 1474, 1343, 1232, 1155, 1044, 972, 922, 865, 778, 728, 680, 621, 573cm^{-1}; ^{1}H

NMR (400MHz, $CDCl_3$, ppm): δ 10.56 (s, 1H), 9.94 (s, 1H), 8.90 (s, 1H), 7.43 (s, 1H), 7.35–7.32 (m, 1H), 7.30 (t, *J* = 7.80Hz, 1H), 7.21 (d, *J* = 7.48Hz, 1H), 2.58 (dd, *J* = 18.56, 3.40Hz, 1H), 2.14 (d, *J* = 14.52Hz, 1H), 2.00–1.32 (m, 14H), 1.27 (s, 3H), 1.25–1.18 (m, 3H), 0.96 (s, 3H), 0.93–0.86 (m, 1H), 0.78 (s, 3H); ^{13}C NMR (100MHz, $CDCl_3$, ppm): δ 222.07, 176.40, 172.10, 138.79, 134.50, 130.00, 126.56, 125.42, 123.50, 57.46, 54.55, 54.03, 48.68, 48.20, 43.14, 41.22, 39.82, 39.37, 38.09, 37.23, 37.16, 30.24, 22.33, 20.32, 19.80, 18.86, 13.74; HRMS (ESI, *m/z*) calcd for $C_{27}H_{37}ClN_3O_2S$ $[M+H]^+$ 502.2295. Found: 502.2293.

4.2.3.10. Compound ***4j***. White powder. Yield 88%; Mp 118.2–120.3 °C; IR (KBr): 3293, 2928, 2848, 1736, 1655, 1595, 1533, 1491, 1338, 1235, 1154, 1090, 1045, 1012, 973, 828, 732, 572, 503cm^{-1}; ^{1}H NMR (400MHz, $CDCl_3$, ppm): δ 10.48 (s, 1H), 9.91 (s, 1H), 8.87 (s, 1H), 7.33 (s, 4H), 2.58 (dd, *J* = 18.56, 3.24Hz, 1H), 2.13 (d, *J* = 14.48Hz, 1H), 1.97–1.33 (m, 14H), 1.27 (s, 3H), 1.25–1.15 (m, 3H), 0.96 (s, 3H), 0.94–0.86 (m, 1H), 0.78 (s, 3H); ^{13}C NMR (100MHz, $CDCl_3$, ppm): δ 222.05, 176.61, 172.09, 136.07, 132.07, 129.25, 129.25, 126.81, 126.81, 57.41, 54.53, 54.01, 48.69, 48.24, 43.11, 41.27, 39.80, 39.37, 38.09, 37.26, 37.15, 30.22, 22.26, 20.31, 19.80, 18.84, 13.73; HRMS (ESI, *m/z*) calcd for $C_{27}H_{37}ClN_3O_2S$ $[M+H]^+$ 502.2295. Found: 502.2293.

4.2.3.11. Compound ***4k***. White powder. Yield 79%; Mp 116.7–118.1 °C; IR (KBr): 3302, 3058, 2928, 2847, 1735, 1655, 1589, 1534, 1465, 1439, 1340, 1294, 1234, 1155, 1027, 974, 855, 754, 732, 663, 622, 572, 516cm^{-1}; ^{1}H NMR (400MHz, $CDCl_3$, ppm): δ 10.55 (s, 1H), 9.98 (s, 1H), 8.80 (s, 1H), 7.65 (d, *J* = 8.04Hz, 1H), 7.62 (d, *J* = 7.96Hz, 1H), 7.38 (t, *J* = 7.66Hz, 1H), 7.18 (t, *J* = 7.72Hz, 1H), 2.55 (dd, *J* = 18.64, 2.92Hz, 1H), 2.14 (d, *J* = 14.76Hz, 1H), 2.02–1.88 (m, 1H), 1.78–1.42 (m, 9H), 1.34–1.31 (m, 2H), 1.29 (s, 3H), 1.25–1.14 (m, 5H), 0.95 (s, 3H), 0.92–0.91 (m, 1H), 0.79 (s, 3H); ^{13}C NMR (100MHz, $CDCl_3$, ppm): δ 222.10, 176.62, 171.65, 136.29, 133.23, 129.38, 128.69, 128.21, 121.55, 57.58, 54.53, 54.02, 48.66, 48.21, 43.12, 41.18, 39.85, 39.28, 38.05, 37.14, 37.14, 30.25, 22.26, 20.30, 19.79, 18.82, 13.78; HRMS (ESI, *m/z*) calcd for $C_{27}H_{37}BrN_3O_2S$ $[M+H]^+$ 546.1790. Found: 546.1785.

4.2.3.12. Compound ***4l***. White powder. Yield 67%; Mp 120.2–121.7 °C; IR (KBr): 3289, 2928, 2847, 1733, 1653, 1590, 1535, 1472, 1344, 1231, 1155, 1044, 974, 863, 776, 733, 678, 621, 573cm^{-1}; ^{1}H NMR (400MHz, $CDCl_3$, ppm): δ 10.50 (s, 1H), 9.95 (s, 1H), 8.91 (s, 1H), 7.56 (t, *J* = 1.70Hz, 1H), 7.38 (d, *J* = 7.96Hz, 2H), 7.25 (t, *J* = 7.24Hz, 1H), 2.58 (dd, *J* = 18.56, 3.24Hz, 1H), 2.14 (d, *J* = 14.56Hz, 1H), 1.99–1.32 (m, 14H), 1.28 (s, 3H), 1.26–1.18 (m, 3H), 0.97 (s, 3H), 0.94–0.90 (m, 1H), 0.78 (s, 3H); ^{13}C NMR (100MHz, $CDCl_3$, ppm): δ 222.05, 176.54, 172.15, 138.89, 130.29, 129.58, 128.43, 124.19, 122.39,

57.45, 54.55, 54.02, 48.68, 48.19, 43.15, 41.19, 39.82, 39.37, 38.09, 37.23, 37.16, 30.24, 22.35, 20.32, 19.80, 18.86, 13.74; HRMS (ESI, *m/z*) calcd for $C_{27}H_{37}BrN_3O_2S$ $[M+H]^+$ 546.1790. Found: 546.1789.

4.2.3.13. Compound ***4m***. White powder. Yield 70%; Mp 124.8–126.6 °C; IR (KBr): 3297, 2929, 2847, 1734, 1655, 1591, 1532, 1488, 1461, 1338, 1280, 1235, 1154, 1072, 1044, 1010, 974, 825, 731, 571, 499cm^{-1}; ^{1}H NMR (400MHz, $CDCl_3$, ppm): δ 10.42 (s, 1H), 9.89 (s, 1H), 8.82 (s, 1H), 7.49 (d, *J* = 8.52Hz, 2H), 7.27 (d, *J* = 8.64Hz, 2H), 2.58 (dd, *J* = 18.56, 3.82Hz, 1H), 2.13 (d, *J* = 14.52Hz, 1H), 1.96–1.33 (m, 14H), 1.27 (s, 3H), 1.25–1.19 (m, 3H), 0.97 (s, 3H), 0.94–0.90 (m, 1H), 0.77 (s, 3H); ^{13}C NMR (100MHz, $CDCl_3$, ppm): δ 222.03, 176.49, 172.16, 136.52, 132.25, 132.25, 127.07, 127.07, 119.98, 57.40, 54.54, 54.01, 48.69, 48.24, 43.13, 41.27, 39.80, 39.38, 38.09, 37.27, 37.15, 30.20, 22.25, 20.32, 19.80, 18.85, 13.73; HRMS (ESI, *m/z*) calcd for $C_{27}H_{37}BrN_3O_2S$ $[M+H]^+$ 546.1790. Found: 546.1787.

4.2.3.14. Compound ***4n***. White powder. Yield 77%; Mp 178.6–179.4 °C; IR (KBr): 3334, 3075, 2930, 2846, 1735, 1603, 1543, 1460, 1357, 1313, 1245, 1154, 1112, 1046, 1025, 974, 927, 857, 789, 747, 698, 574, 503cm^{-1}; ^{1}H NMR (400MHz, $CDCl_3$, ppm): δ 9.56 (s, 2H), 8.01 (s, 1H), 7.65 (s, 1H), 7.21 (t, *J* = 7.70Hz, 1H), 7.00 (t, *J* = 7.18Hz, 1H), 6.95 (d, *J* = 8.12Hz, 1H), 3.85 (s, 3H), 2.60 (d, *J* = 18.64Hz, 1H), 2.15 (d, *J* = 14.88Hz, 1H), 2.00–1.89 (m, 2H), 1.81–1.50 (m, 9H), 1.45–1.32 (m, 3H), 1.26 (s, 3H), 1.24–1.15 (m, 4H), 0.96 (s, 3H), 0.76 (s, 3H); ^{13}C NMR (100MHz, $CDCl_3$, ppm): δ 222.29, 176.94, 171.21, 144.53, 127.41, 125.73, 124.30, 121.16, 111.56, 57.55, 55.73, 54.61, 54.14, 48.69, 48.31, 43.12, 41.45, 39.91, 39.41, 38.07, 37.20, 37.20, 30.01, 21.98, 20.31, 19.83, 18.94, 13.72; HRMS (ESI, *m/z*) calcd for $C_{28}H_{40}N_3O_3S$ $[M+H]^+$ 498.2790. Found: 498.2804.

4.2.3.15. Compound ***4o***. White powder. Yield 89%; Mp 98.4–100.2 °C; IR (KBr): 3298, 3054, 2930, 2846, 1735, 1654, 1602, 1538, 1461, 1351, 1229, 1156, 1087, 1044, 973, 900, 860, 775, 690, 627, 571, 455cm^{-1}; ^{1}H NMR (400MHz, $CDCl_3$, ppm): δ 10.02 (s, 1H), 9.74 (s, 1H), 8.62 (s, 1H), 7.29 (t, *J* = 7.82Hz, 1H), 6.96 (s, 1H), 6.93 (d, *J* = 7.80Hz, 1H), 6.79 (d, *J* = 8.20Hz, 1H), 3.79 (s, 3H), 2.58 (dd, *J* = 18.64, 3.00Hz, 1H), 2.15 (d, *J* = 17.48Hz, 1H), 2.00–1.32 (m, 13H), 1.27 (s, 3H), 1.24–1.17 (m, 4H), 0.96 (s, 3H), 0.94–0.87 (m, 1H), 0.77 (s, 3H); ^{13}C NMR (100MHz, $CDCl_3$, ppm): δ 222.22, 175.95, 172.24, 160.34, 138.02, 130.20, 117.03, 112.63, 110.72, 57.49, 55.44, 54.58, 54.09, 48.68, 48.25, 43.11, 41.34, 39.87, 39.38, 38.08, 37.25, 37.18, 30.16, 22.15, 20.31, 19.82, 18.91, 13.74; HRMS (ESI, *m/z*) calcd for $C_{28}H_{40}N_3O_3S$ $[M+H]^+$ 498.2790. Found: 498.2830.

4.2.3.16. Compound ***4p***. White powder. Yield 72%; Mp 112.2–112.8 °C; IR (KBr): 3291, 3050, 2930, 2846, 1736, 1653, 1602, 1512, 1463, 1347, 1297, 1246, 1172, 1110, 1033, 973, 830, 733, 695, 586, 517cm^{-1}; ^{1}H

NMR (400MHz, $CDCl_3$, ppm): δ 9.81 (s, 2H), 8.52 (s, 1H), 7.25 (d, J = 8.84Hz, 2H), 6.92 (d, J = 8.40Hz, 2H), 3.81 (s, 3H), 2.68 (dd, J = 18.64, 2.52Hz, 1H), 2.12 (d, J = 14.52Hz, 1H), 1.96–1.35 (m, 13H), 1.25 (s, 3H), 1.24–1.16 (m, 4H), 0.96 (s, 3H), 0.92–0.90 (m, 1H), 0.77 (s, 3H); ^{13}C NMR (100MHz, $CDCl_3$, ppm): δ 222.15, 176.63, 171.74, 158.61, 129.41, 127.53, 127.53, 114.74, 114.74, 57.49, 55.49, 54.46, 54.08, 48.67, 48.25, 43.02, 41.34, 39.86, 39.37, 38.06, 37.18, 37.18, 30.17, 22.16, 20.30, 19.82, 18.87, 13.73; HRMS (ESI, *m/z*) calcd for $C_{28}H_{40}N_3O_3S$ $[M+H]^+$ 498.2790. Found: 498.2787.

4.2.3.17. Compound ***4q***. Yellow powder. Yield 70%; Mp 111.4–115.6 °C; IR (KBr): 3297, 2930, 2849, 1735, 1665, 1608, 1586, 1510, 1457, 1347, 1267, 1165, 1110, 1086, 976, 857, 741, 511cm^{-1}; ^{1}H NMR (400MHz, $CDCl_3$, ppm): δ 10.10 (s, 1H), 8.43 (s, 1H), 8.02 (d, J = 8.32Hz, 1H), 7.54 (t, J = 7.76Hz, 1H), 7.18 (t, J = 7.24Hz, 1H), 2.87 (d, J = 32.84Hz, 1H), 2.51 (dd, J = 18.60, 3.24Hz, 1H), 2.14 (d, J = 14.12Hz, 1H), 1.87–1.28 (m, 14H), 1.25 (s, 3H), 1.21–1.11 (m, 4H), 0.89 (s, 3H), 0.69 (s, 3H); ^{13}C NMR (100MHz, $CDCl_3$, ppm): δ 222.47, 179.82, 173.19, 139.99, 134.29, 133.90, 126.01, 125.46, 124.88, 57.56, 54.61, 54.10, 48.72, 48.30, 41.42, 39.84, 39.42, 38.09, 37.34, 37.19, 29.86, 22.05, 20.32, 19.80, 19.00, 13.82; HRMS (ESI, *m/z*) calcd for $C_{27}H_{37}N_4O_4S$ $[M+H]^+$ 513.2536. Found:513.2532.

4.2.3.18. Compound ***4r***. Yellow powder. Yield 72%; Mp 124.0–126.4 °C; IR (KBr): 3309, 3095, 2930, 2848, 1736, 1659, 1616, 1529, 1467, 1347, 1247, 1155, 1090, 1045, 974, 888, 830, 799, 735, 672, 587, 509cm^{-1}; ^{1}H NMR (400MHz, $CDCl_3$, ppm): δ 10.72 (s, 1H), 9.84 (s, 1H), 9.21 (s, 1H), 8.31 (t, J = 4.00Hz, 1H), 8.06 (dd, J = 8.24, 1.36Hz, 1H), 7.87 (dd, J = 8.04, 1.20Hz, 1H), 7.52 (t, J = 8.16Hz, 1H), 2.58 (dd, J = 18.56, 3.40Hz, 1H), 2.17 (d, J = 14.36Hz, 1H), 1.94–1.36 (m, 13H), 1.33 (s, 3H), 1.29–1.20 (m, 4H), 0.97 (s, 3H), 0.94–0.93 (m, 1H), 0.80 (s, 3H); ^{13}C NMR (100MHz, $CDCl_3$, ppm): δ 222.17, 177.00, 173.18, 148.28, 139.15, 130.93, 129.51, 120.71, 119.71, 57.38, 54.50, 53.93, 48.71, 48.23, 43.31, 41.19, 39.75, 39.39, 38.13, 37.33, 37.13, 30.22, 22.34, 20.32, 19.78, 18.86, 13.77; HRMS (ESI, *m/z*) calcd for $C_{27}H_{37}N_4O_4S$ $[M+H]^+$ 513.2536. Found:513.2532.

4.2.3.19. Compound ***4s***. Yellow powder. Yield 50%; Mp 137.7–140.1 °C; IR (KBr): 3312, 3112, 2929, 2848, 1735, 1659, 1595, 1548, 1512, 1465, 1330, 1246, 1179, 1111, 1044, 973, 852, 731, 698, 587, 530, 493cm^{-1}; ^{1}H NMR (400MHz, $CDCl_3$, ppm): δ 10.54 (s, 1H), 9.61 (s, 1H), 9.19 (s, 1H), 8.19 (d, J = 9.08Hz, 2H), 7.71 (d, J = 9.04Hz, 2H), 2.58 (dd, J = 18.56, 3.28Hz, 1H), 2.18 (d, J = 14.28Hz, 1H), 1.95–1.38 (m, 12H), 1.33 (s, 3H), 1.29–1.21 (m, 5H), 0.97 (s, 3H), 0.94–0.92 (m, 1H), 0.77 (s, 3H); ^{13}C NMR (100MHz, $CDCl_3$, ppm): δ 222.45, 178.86, 171.27, 134.27, 134.01, 125.46, 125.46, 124.75, 124.75, 57.53, 54.57, 54.06, 48.70, 48.28, 43.49, 41.39, 39.80, 39.39, 38.07, 37.28, 37.16, 29.89, 22.01, 20.29, 19.79, 18.95,

13.77; HRMS (ESI, *m/z*) calcd for $C_{27}H_{37}N_4O_4S$ $[M+H]^+$ 513.2536. Found:513.2532.

4.2.3.20. Compound ***4t****.* White powder. Yield 75%; Mp 126.4–127.9 °C; IR (KBr): 3309, 3087, 2929, 2847, 1735, 1659, 1581, 1530, 1468, 1370, 1336, 1295, 1231, 1152, 1103, 1050, 974, 861, 813, 780, 735, 573cm^{-1}; ^{1}H NMR (400MHz, $CDCl_3$, ppm): δ 10.75 (s, 1H), 9.95 (s, 1H), 8.82 (s, 1H), 7.65 (d, *J* = 7.88Hz, 1H), 7.47 (d, *J* = 2.28Hz, 1H), 7.30 (dd, *J* = 8.64, 2.36Hz, 1H), 2.57 (dd, *J* = 18.56, 3.40Hz, 1H), 2.12 (d, *J* = 14.56Hz, 1H), 1.97–1.87 (m, 1H), 1.78–1.46 (m, 9H), 1.37–1.35 (m, 3H), 1.27 (s, 3H), 1.26–1.16 (m, 4H), 0.96 (s, 3H), 0.93–0.90 (m, 1H), 0.78 (s, 3H); ^{13}C NMR (100MHz, $CDCl_3$, ppm): δ 222.09, 176.70, 171.94, 133.74, 132.98, 131.25, 129.89, 129.65, 127.62, 57.44, 54.47, 53.95, 48.66, 48.20, 43.12, 41.22, 39.77, 39.29, 38.04, 37.16, 37.11, 30.13, 22.13, 20.28, 19.76, 18.74, 13.72; HRMS (ESI, *m/z*) calcd for $C_{27}H_{36}Cl_2N_3O_2S[M+H]^+$ 536.1905. Found: 536.1902.

4.2.3.21. Compound ***4u****.* White powder. Yield 58%; Mp 126.2–127.3 °C; IR (KBr): 3279, 3037, 2926, 2847, 1738, 1632, 1523, 1469, 1372, 1337, 1236, 1163, 1111, 1090, 1036, 973, 922, 772, 735, 676, 584, 509cm^{-1}; ^{1}H NMR (400MHz, $CDCl_3$, ppm): δ 10.09 (s, 1H), 8.31 (s, 1H), 8.11 (dd, *J* = 8.32, 1.16Hz, 1H), 8.03 (s, 1H), 7.62 (t, *J* = 7.80Hz, 1H), 7.25 (d, *J* = 7.00Hz, 1H), 2.99 (s, 3H), 2.91 (s, 3H), 2.58 (dd, *J* = 18.64, 3.28Hz, 1H), 2.20 (d, *J* = 13.92Hz, 1H), 1.95–1.92 (m, 2H), 1.85–1.45 (m, 9H), 1.41–1.35 (m, 2H), 1.32 (s, 3H), 1.29–1.19 (m, 5H), 0.96 (s, 3H), 0.77 (s, 3H); ^{13}C NMR (100MHz, $CDCl_3$, ppm): δ 222.57, 176.51, 174.15, 144.25, 144.05, 124.58, 124.58, 122.87, 122.87, 58.48, 57.38, 54.48, 53.92, 48.76, 48.30, 43.42, 41.27, 39.73, 39.43, 38.15, 37.35, 37.13, 30.12, 22.21, 20.33, 19.77, 18.92, 18.40, 13.74; HRMS (ESI, *m/z*) calcd for $C_{29}H_{42}N_3O_2S[M+H]^+$ 496.2998. Found: 496.2994.

4.2.4. General procedure for synthesis of compounds 5a-5u

Compound **4a-4u** (1 mmol) was dissolved in EtOH (20 mL), and $Hg(OAc)_2$ (0.351 g, 1.1 mmol) was added.The mixture was stirred at reflux for 8 h. The reaction mixture was filtered and concentrated under reduced pressure. The residue was diluted with saturated NaCl aqueous solution and extracted with $CH_3CO_2C_2H_5$. The combined organic layer was dried over anhydrous sodium sulfate, filtered and concentrated. The residue was purified on silica gel column to give the corresponding product **5a-5u**.

4.2.4.1. Compound ***5a****.* White solid. Yield 97%; Mp 115.2–116.3 °C; IR (KBr): 3298, 3137, 3087, 2925, 2849, 1735, 1626, 1599, 1559, 1499, 1451, 1373, 1319, 1243, 1172, 1132, 1082, 1049, 972, 856, 751, 692, 505cm^{-1}; ^{1}H NMR (400MHz, $CDCl_3$, ppm): δ 8.27 (s, 1H), 7.46 (d, *J* = 7.68Hz, 2H), 7.32 (t, *J* = 7.74Hz, 2H), 7.04 (t, *J* = 7.30Hz, 1H), 2.58 (dd, *J* = 18.60, 3.56Hz, 1H), 2.51 (d, *J* = 13.40Hz, 1H), 2.12–1.97 (m, 2H), 1.78–1.51 (m, 9H), 1.44–1.34 (m, 3H), 1.31 (s, 3H), 1.27–1.01 (m, 4H), 0.97 (s, 3H), 0.52 (s, 3H);

^{13}C NMR (100MHz, $CDCl_3$, ppm): δ 222.25, 165.43, 159.88, 138.17, 129.32, 129.32, 122.75, 117.38, 117.38, 57.06, 54.69, 54.27, 48.72, 48.44, 41.26, 39.58, 39.35, 38.26, 37.85, 37.51, 37.18, 30.01, 21.47, 20.16, 19.83, 18.51, 13.05; HRMS (ESI, *m/z*) calcd for $C_{27}H_{36}N_3O_2$ $[M+H]^+$ 434.2808. Found: 434.2804.

4.2.4.2. Compound ***5b***. White solid. Yield 70%; Mp 198.4–200.5 °C; IR (KBr): 3444, 3058, 2924, 2850, 1736, 1626, 1598, 1558, 1458, 1374, 1249, 1090, 975, 857, 750, 546cm^{-1}; ^{1}H NMR (400MHz, $CDCl_3$, ppm): δ 7.77 (d, *J* = 7.92Hz, 1H), 7.30 (s, 1H), 7.26 (d, *J* = 7.64Hz, 1H), 7.21 (t, *J* = 7.12Hz, 1H), 7.02 (td, *J* = 7.40, 0.76Hz, 1H), 2.59 (dd, *J* = 18.60, 7.68Hz, 1H), 2.50 (d, *J* = 13.52Hz, 1H), 2.36 (s, 3H), 2.13–1.94 (m, 2H), 1.80–1.52 (m, 9H), 1.41–1.34 (m, 3H), 1.30 (s, 3H), 1.27–1.13 (m, 4H), 0.97 (s, 3H), 0.54 (s, 3H); ^{13}C NMR (100MHz, $CDCl_3$, ppm): δ 222.22, 165.57, 160.28, 136.41, 130.70, 127.09, 126.52, 123.51, 118.68, 57.01, 54.67, 54.27, 48.71, 48.44, 41.23, 39.59, 39.35, 38.25, 37.85, 37.51, 37.19, 30.03, 21.42, 20.16, 19.85, 18.52, 17.83, 13.10; HRMS (ESI, *m/z*) calcd for $C_{28}H_{38}N_3O_2$ $[M+H]^+$ 448.2964. Found: 448.2960.

4.2.4.3. Compound ***5c***. White solid. Yield 37%; Mp 108.6–109.1 °C; IR (KBr):3295, 3090, 2929, 2850, 1737, 1629, 1601, 1561, 1493, 1454, 1374, 1318, 1256, 1229, 1131, 1052, 975, 932, 866, 778, 691cm^{-1}; ^{1}H NMR (400MHz, $CDCl_3$, ppm): δ 7.33 (s, 1H), 7.23–7.17 (m, 3H), 6.88 (d, *J* = 6.80Hz, 1H), 2.58 (dd, *J* = 18.56, 3.56Hz, 1H), 2.50 (d, *J* = 13.48Hz, 1H), 2.34 (s, 3H), 2.11–1.98 (m, 2H), 1.79–1.53 (m, 9H), 1.48–1.35 (m, 3H), 1.32 (s, 3H), 1.22–1.13 (m, 4H), 0.97 (s, 3H), 0.53 (s, 3H); ^{13}C NMR (100MHz, $CDCl_3$, ppm): δ 222.16, 165.31, 159.61, 139.31, 137.65, 129.15, 123.92, 118.29, 114.78, 57.01, 54.66, 54.27, 48.70, 48.43, 41.24, 39.53, 39.32, 38.19, 37.82, 37.52, 37.14, 29.97, 21.58, 21.48, 20.14, 19.81, 18.43, 13.04; HRMS (ESI, *m/z*) calcd for $C_{28}H_{38}N_3O_2$ $[M+H]^+$ 448.2964. Found: 448.2960.

4.2.4.4. Compound ***5d***. White solid. Yield 25%; Mp 101.2–103.4 °C; IR (KBr): 3291, 3063, 2928, 2850, 1737, 1629, 1560, 1516, 1455, 1374, 1248, 1173, 1130, 1051, 974, 816, 506cm^{-1}; ^{1}H NMR (400MHz, $CDCl_3$, ppm): δ 7.88 (s, 1H), 7.32 (d, *J* = 8.44Hz, 2H), 7.13 (d, *J* = 8.32Hz, 2H), 2.58 (dd, *J* = 18.60, 3.64Hz, 1H), 2.50 (d, *J* = 13.48Hz, 1H), 2.31 (s, 3H), 2.04–1.96 (m, 2H), 1.79–1.52 (m, 9H), 1.45–1.34 (m, 3H), 1.31 (s, 3H), 1.28–1.19 (m, 4H), 0.97 (s, 3H), 0.52 (s, 3H); ^{13}C NMR (100MHz, $CDCl_3$, ppm): δ 222.26, 165.29, 159.97, 135.49, 132.39, 129.82, 129.82, 117.51, 117.51, 57.02, 54.66, 54.25, 48.70, 48.42, 41.24, 39.56, 39.33, 38.23, 37.82, 37.47, 37.16, 29.98, 21.44, 20.70, 20.14, 19.82, 18.49, 13.04; HRMS (ESI, *m/z*) calcd for $C_{28}H_{38}N_3O_2$ $[M+H]^+$ 448.2964. Found: 448.2961.

4.2.4.5. Compound ***5e***. White solid. Yield 38%; Mp 91.7–93.6 °C; IR (KBr): 3286, 3070, 2929, 2848, 1735, 1625, 1591, 1559, 1495, 1458, 1373, 1337, 1255, 1131, 1049, 974, 928, 873, 794, 752, 572cm^{-1}; ^{1}H NMR

(400MHz, $CDCl_3$, ppm): δ 8.22 (td, J = 8.36, 1.32Hz, 1H), 7.16 (t, J = 7.92Hz, 1H), 7.14–7.09 (m, 1H), 7.02–6.97 (m, 1H), 2.60 (dd, J = 18.60, 3.68Hz, 1H), 2.51 (d, J = 13.56Hz, 1H), 2.17–1.98 (m, 2H), 1.82–1.53 (m, 9H), 1.45–1.36 (m, 3H), 1.32 (s, 3H), 1.30–1.20 (m, 4H), 0.97 (s, 3H), 0.53 (s, 3H); ^{13}C NMR (100MHz, $CDCl_3$, ppm): δ 222.16, 165.84, 158.89, 151.58 (d, J = 241.00Hz), 126.32 (d, J = 10.35Hz), 124.90 (d, J = 3.68Hz), 122.89 (d, J = 7.24Hz), 118.77, 114.85 (d, J = 18.34Hz), 57.01, 54.70, 54.27, 48.70, 48.47, 41.20, 39.54, 39.34, 38.24, 37.85, 37.49, 37.17, 29.99, 21.51, 20.15, 19.83, 18.49, 13.03; HRMS (ESI, *m/z*) calcd for $C_{27}H_{35}FN_3O_2$ $[M+H]^+$ 452.2713. Found: 452.2709.

4.2.4.6. Compound ***5f***. White solid. Yield 22%; Mp 118.7–121.5 °C; IR (KBr): 3280, 3152, 3094, 2927, 2849, 1735, 1614, 1559, 1493, 1454, 1373, 1256, 1173, 1149, 1051, 951, 862, 775, 682, 573cm^{-1}; ^{1}H NMR (400MHz, $CDCl_3$, ppm): δ 8.70 (s, 1H), 7.33–7.28 (m, 2H), 7.14 (dd, J = 8.12, 1.40Hz, 1H), 6.74 (td, J = 8.32, 2.12Hz, 1H), 2.58 (dd, J = 18.60, 3.64Hz, 1H), 2.52 (d, J = 13.52Hz, 1H), 2.10–2.00 (m, 2H), 1.80–1.53 (m, 9H), 1.45–1.36 (m, 3H), 1.33 (s, 3H), 1.25–1.16 (m, 4H), 0.97 (s, 3H), 0.52 (s, 3H); ^{13}C NMR (100MHz, $CDCl_3$, ppm): δ 222.32, 165.69, 163.39 (d, J = 243.59Hz), 159.53, 139.62 (d, J = 10.89Hz), 130.55 (d, J = 9.45Hz), 112.91, 109.43 (d, J = 21.21Hz), 104.66 (d, J = 26.76Hz), 57.01, 54.64, 54.21, 48.72, 48.40, 41.20, 39.52, 39.34, 38.21, 37.84, 37.55, 37.15, 29.99, 21.50, 20.14, 19.81, 18.46, 13.04; HRMS (ESI, *m/z*) calcd for $C_{27}H_{35}FN_3O_2$ $[M+H]^+$ 452.2713. Found: 452.2710.

4.2.4.7. Compound ***5g***. White solid. Yield 58%; Mp 185.5–187.2 °C; IR (KBr): 3293, 3159, 3087, 2929, 2849, 1735, 1627, 1563, 1509, 1454, 1419, 1374, 1222, 1131, 1051, 973, 833, 807, 619, 555, 511cm^{-1}; ^{1}H NMR (400MHz, $CDCl_3$, ppm): δ 8.29 (s, 1H), 7.41 (d, J = 9.04Hz, 1H), 7.40 (d, J = 9.08Hz, 1H), 7.04 (d, J = 8.56Hz, 1H), 7.02 (d, J = 8.72Hz, 1H), 2.58 (dd, J = 18.56, 3.64Hz, 1H), 2.48 (d, J = 13.52Hz, 1H), 2.10–1.96 (m, 2H), 1.79–1.52 (m, 9H), 1.45–1.35 (m, 3H), 1.31 (s, 3H), 1.25–1.17 (m, 4H), 0.97 (s, 3H), 0.52 (s, 3H); ^{13}C NMR (100MHz, $CDCl_3$, ppm): δ 222.30, 165.39, 159.91, 158.62 (d, J = 240.55Hz), 134.17, 119.12 (d, J = 7.83Hz), 119.12 (d, J = 7.83Hz), 115.99 (d, J = 22.61Hz), 115.99 (d, J = 22.61Hz), 57.01, 54.64, 54.23, 48.73, 48.42, 41.23, 39.53, 39.34, 38.21, 37.83, 37.51, 37.16, 29.99, 21.45, 20.15, 19.83, 18.48, 13.05; HRMS (ESI, *m/z*) calcd for $C_{27}H_{35}FN_3O_2$ $[M+H]^+$ 452.2713. Found: 452.2710.

4.2.4.8. Compound ***5h***. White solid. Yield 26%; Mp 186.4–188.4 °C; IR (KBr): 3360, 3074, 2920, 2849, 1731, 1616, 1552, 1523, 1474, 1444, 1399, 1373, 1309, 1269, 1229, 1170, 1131, 1110, 1052, 974, 927, 857, 744, 711, 465cm^{-1}; ^{1}H NMR (400MHz, $CDCl_3$, ppm): δ 8.33 (dd, J = 8.32, 1.36Hz, 1H), 7.40 (dd, J = 8.00, 1.40Hz, 1H), 7.32 (td, J = 8.72, 1.44Hz, 1H), 7.00 (td, J = 7.70, 1.44Hz, 1H), 2.61 (dd, J = 18.56, 3.72Hz, 1H), 2.51 (d, J = 13.56Hz, 1H), 2.17–1.99 (m, 2H), 1.83–1.53 (m, 9H), 1.45–1.35 (m, 3H), 1.33 (s, 3H),

1.31–1.15 (m, 4H), 0.97 (s, 3H), 0.54 (s, 3H); ^{13}C NMR (100MHz, $CDCl_3$, ppm): δ 222.09, 165.94, 158.73, 134.38, 129.14, 128.13, 123.17, 120.84, 118.20, 56.97, 54.70, 54.26, 48.68, 48.47, 41.16, 39.50, 39.31, 38.27, 37.84, 37.50, 37.15, 30.01, 21.53, 20.13, 19.82, 18.50, 13.06; HRMS (ESI, *m/z*) calcd for $C_{27}H_{35}ClN_3O_2$ $[M+H]^+$ 468.2418. Found: 468.2416.

4.2.4.9. Compound ***5i***. White solid. Yield 19%; Mp 116.8–118.6 °C; IR (KBr): 3282, 3088, 2926, 2849, 1735, 1626, 1597, 1557, 1481, 1452, 1372, 1317, 1253, 1131, 1051, 974, 909, 871, 776, 733, 683, 619, 572cm^{-1}; ^{1}H NMR (400MHz, $CDCl_3$, ppm): δ 8.96 (s, 1H), 7.55 (s, 1H), 7.26–7.24 (m, 2H), 7.03–7.00 (m, 1H), 2.56 (dd, *J* = 18.60, 3.64Hz, 1H), 2.52 (d, *J* = 13.56Hz, 1H), 2.13–2.01 (m, 2H), 1.82–1.53 (m, 9H), 1.45–1.34 (m, 3H), 1.33 (s, 3H), 1.26–1.13 (m, 4H), 0.97 (s, 3H), 0.52 (s, 3H); ^{13}C NMR (100MHz, $CDCl_3$, ppm): δ 222.36, 165.70, 159.64, 139.25, 135.04, 130.37, 122.73, 117.18, 115.63, 57.02, 54.64, 54.18, 48.72, 48.43, 41.21, 39.53, 39.36, 38.18, 37.83, 37.57, 37.14, 29.98, 21.57, 20.14, 19.81, 18.43, 13.02; HRMS (ESI, *m/z*) calcd for $C_{27}H_{35}ClN_3O_2$ $[M+H]^+$ 468.2418. Found: 468.2416.

4.2.4.10. Compound ***5j***. White solid. Yield 10%; Mp 126.7–129.2 °C; IR (KBr): 3286, 3077, 2923, 2849, 1735, 1624, 1558, 1493, 1454, 1409, 1373, 1320, 1245, 1173, 1130, 1093, 1051, 972, 925, 828, 732, 504cm^{-1}; ^{1}H NMR (400MHz, $CDCl_3$, ppm): δ 8.72 (s, 1H), 7.41 (d, *J* = 8.88Hz, 2H), 7.29 (d, *J* = 8.88Hz, 2H), 2.57 (dd, *J* = 18.56, 3.56Hz, 1H), 2.48 (d, *J* = 13.52Hz, 1H), 2.09–1.97 (m, 2H), 1.79–1.52 (m, 9H), 1.43–1.36 (m, 3H), 1.31 (s, 3H), 1.26–1.12 (m, 4H), 0.97 (s, 3H), 0.51 (s, 3H); ^{13}C NMR (100MHz, $CDCl_3$, ppm): δ 222.36, 165.55, 159.60, 136.69, 129.29, 129.29, 127.70, 118.57, 118.57, 56.97, 54.59, 54.18, 48.71, 48.40, 41.18, 39.48, 39.32, 38.19, 37.80, 37.50, 37.13, 29.97, 21.43, 20.12, 19.80, 18.45, 13.03; HRMS (ESI, *m/z*) calcd for $C_{27}H_{35}ClN_3O_2$ $[M+H]^+$ 468.2418. Found: 468.2413.

4.2.4.11. Compound ***5k***. White solid. Yield 91%; Mp 196.8–198.5 °C; IR (KBr): 3389, 3289, 3066, 2929, 2847, 1735, 1618, 1555, 1443, 1401, 1371, 1314, 1268, 1129, 1049, 1024, 972, 928, 750, 702, 572cm^{-1}; ^{1}H NMR (400MHz, $CDCl_3$, ppm): δ 8.32 (dd, *J* = 8.32, 1.40Hz, 1H), 7.56 (dd, *J* = 8.00, 1.36Hz, 1H), 7.36 (td, *J* = 7.86, 1.44Hz, 1H), 6.93 (td, *J* = 7.68, 1.48Hz, 1H), 2.61 (dd, *J* = 18.60, 3.72Hz, 1H), 2.50 (d, *J* = 13.56Hz, 1H), 2.15–1.99 (m, 2H), 1.83–1.53 (m, 9H), 1.41–1.35 (m, 3H), 1.33 (s, 3H), 1.31–1.13 (m, 4H), 0.97 (s, 3H), 0.54 (s, 3H); ^{13}C NMR (100MHz, $CDCl_3$, ppm): δ 222.16, 165.98, 158.79, 135.50, 132.43, 128.82, 123.70, 118.41, 111.31, 56.98, 54.70, 54.27, 48.69, 48.48, 41.17, 39.51, 39.33, 38.28, 37.85, 37.52, 37.17, 30.04, 21.53, 20.15, 19.84, 18.53, 13.09; HRMS (ESI, *m/z*) calcd for $C_{27}H_{35}BrN_3O_2$ $[M+H]^+$ 512.1913. Found: 512.1908.

4.2.4.12. Compound ***5l***. White solid. Yield 88%; Mp 126.2–128.4 °C; IR (KBr): 3282, 3090, 2934, 2849,

1735, 1625, 1595, 1556, 1480, 1454, 1373, 1319, 1251, 1172, 1051, 975, 894, 774, 681cm^{-1}; ^{1}H NMR (400MHz, $CDCl_3$, ppm): δ 7.69 (s, 1H), 7.28–7.25 (m, 1H), 7.20–7.19 (m, 2H), 2.56 (dd, *J* = 18.60, 3.56Hz, 1H), 2.50 (d, *J* = 13.52Hz, 1H), 2.06–2.01 (m, 2H), 1.84–1.51 (m, 10H), 1.41–1.35 (m, 3H), 1.33 (s, 3H), 1.26–1.12 (m, 3H), 0.97 (s, 3H), 0.51 (s, 3H); ^{13}C NMR (100MHz, $CDCl_3$, ppm): δ 222.32, 165.65, 159.83, 138.99, 130.71, 126.00, 123.04, 120.16, 116.46, 56.99, 54.60, 54.12, 48.70, 48.40, 41.15, 39.47, 39.35, 38.06, 37.81, 37.60, 37.11, 29.91, 21.58, 20.12, 19.80, 18.38, 13.02; HRMS (ESI, *m/z*) calcd for $C_{27}H_{35}BrN_3O_2$ $[M+H]^+$ 512.1913. Found: 512.1907.

4.2.4.13. Compound ***5m***. White solid. Yield 95%; Mp 133.1–135.2 °C; IR (KBr): 3284, 3186, 3124, 3074, 2935, 2849, 1735, 1624, 1594, 1558, 1491, 1454, 1407, 1373, 1319, 1245, 1175, 1131, 1074, 1051, 1009, 974, 825, 501cm^{-1}; ^{1}H NMR (400MHz, $CDCl_3$, ppm): δ 8.45 (s, 1H), 7.44 (d, *J* = 8.88Hz, 2H), 7.36 (d, *J* = 8.88Hz, 2H), 2.58 (dd, *J* = 18.52, 3.56Hz, 1H), 2.49 (d, *J* = 13.52Hz, 1H), 2.12–1.97 (m, 2H), 1.79–1.52 (m, 9H), 1.45–1.36 (m, 3H), 1.31 (s, 3H), 1.26–1.12 (m, 4H), 0.97 (s, 3H), 0.51 (s, 3H); ^{13}C NMR (100MHz, $CDCl_3$, ppm): δ 222.33, 165.60, 159.49, 137.16, 132.22, 132.22, 118.90, 118.90, 115.13, 56.97, 54.60, 54.19, 48.71, 48.40, 41.18, 39.48, 39.32, 38.19, 37.81, 37.49, 37.13, 29.98, 21.44, 20.12, 19.81, 18.45, 13.03; HRMS (ESI, *m/z*) calcd for $C_{27}H_{35}BrN_3O_2$ $[M+H]^+$ 512.1913. Found: 512.1908.

4.2.4.14. Compound ***5n***. White solid. Yield 44%; Mp 162.3–164.1 °C; IR (KBr): 3400, 3082, 2957, 2909, 2842, 1738, 1624, 1592, 1559, 1528, 1488, 1462, 1345, 1249, 1216, 1176, 1120, 974, 928, 748, 475cm^{-1}; ^{1}H NMR (400MHz, $CDCl_3$, ppm): δ 8.10 (t, *J* = 4.62Hz, 1H), 7.52 (s, 1H), 7.02–6.98 (m, 2H), 6.93–6.89 (m, 1H), 3.94 (s, 3H), 2.60 (dd, *J* = 18.60, 3.68Hz, 1H), 2.51 (d, *J* = 13.52Hz, 1H), 2.17–1.99 (m, 2H), 1.81–1.52 (m, 9H), 1.42–1.35 (m, 3H), 1.31 (s, 3H), 1.24–1.13 (m, 4H), 0.97 (s, 3H), 0.53 (s, 3H); ^{13}C NMR (100MHz, $CDCl_3$, ppm): δ 222.27, 165.36, 159.40, 146.99, 127.35, 124.41, 121.27, 116.78, 109.98, 57.00, 55.76, 54.67, 54.25, 48.69, 48.45, 41.21, 39.54, 39.31, 38.24, 37.82, 37.43, 37.15, 29.97, 21.49, 20.12, 19.82, 18.50, 13.01; HRMS (ESI, *m/z*) calcd for $C_{28}H_{38}N_3O_3$ $[M+H]^+$ 464.2913. Found: 464.2910.

4.2.4.15. Compound ***5o***. White solid. Yield 57%; Mp 110.5–113.1 °C; IR (KBr): 3292, 3091, 2937, 2849, 1735, 1629, 1599, 1559, 1497, 1456, 1285, 1161, 975, 852, 771, 689cm^{-1}; ^{1}H NMR (400MHz, $CDCl_3$, ppm): δ 8.76 (s, 1H), 7.21 (t, *J* = 8.18Hz, 1H), 7.18 (s, 1H), 6.92 (d, *J* = 8.00Hz, 1H), 6.60 (dd, *J* = 8.12, 1.48Hz, 1H), 3.82 (s, 3H), 2.58 (dd, *J* = 18.56, 3.28Hz, 1H), 2.50 (d, *J* = 13.44Hz, 1H), 2.14–1.99 (m, 2H), 1.79–1.52 (m, 9H), 1.48–1.35 (m, 3H), 1.32 (s, 3H), 1.26–1.13 (m, 4H), 0.97 (s, 3H), 0.53 (s, 3H); ^{13}C NMR (100MHz, $CDCl_3$, ppm): δ 222.39, 165.47, 160.58, 159.91, 139.38, 130.07, 109.51, 108.68, 102.94, 57.01, 55.29, 54.65, 54.23, 48.73, 48.45, 41.24, 39.55, 39.34, 38.25, 37.84, 37.52, 37.16, 30.02, 21.52,

20.15, 19.84, 18.50, 13.05; HRMS (ESI, *m/z*) calcd for $C_{28}H_{38}N_3O_3$ $[M+H]^+$ 464.2913. Found: 464.2910.

4.2.4.16. Compound ***5p***. White solid. Yield 64%; Mp 71.8–74.3 °C; IR (KBr): 3284, 3072, 2934, 2849, 1735, 1628, 1563, 1512, 1456, 1373, 1242, 1176, 1035, 974, 829, 592, 518cm^{-1}; ^1H NMR (400MHz, $CDCl_3$, ppm): δ 7.89 (s, 1H), 7.36 (d, *J* = 8.96Hz, 2H), 6.88 (d, *J* = 9.00Hz, 2H), 3.79 (s, 3H), 2.57 (dd, *J* = 18.56, 3.60Hz, 1H), 2.48 (d, *J* = 13.48Hz, 1H), 2.12–1.94 (m, 2H), 1.78–1.50 (m, 9H), 1.44–1.33 (m, 3H), 1.29 (s, 3H), 1.24–1.13 (m, 4H), 0.97 (s, 3H), 0.52 (s, 3H); ^{13}C NMR (100MHz, $CDCl_3$, ppm): δ 222.36, 165.17, 160.26, 155.57, 131.31, 119.50, 119.50, 114.50, 114.50, 57.00, 55.55, 54.62, 54.21, 48.71, 48.41, 41.22, 39.55, 39.32, 38.19, 37.81, 37.44, 37.15, 29.97, 21.40, 20.13, 19.82, 18.47, 13.03; HRMS (ESI, *m/z*) calcd for $C_{28}H_{38}N_3O_3$ $[M+H]^+$ 464.2913. Found: 464.2913.

4.2.4.17. Compound ***5q***. Pale yellow solid. Yield 50%; Mp 163.6–165.3 °C; IR (KBr): 3325, 2941, 2849, 1735, 1691, 1600, 1551, 1505, 1448, 1347, 1268, 1149, 1054, 979, 878, 783, 743, 584cm^{-1}; ^1H NMR (400MHz, $CDCl_3$, ppm): δ 10.58 (s, 1H), 8.80 (d, *J* = 8.60Hz, 1H), 8.31 (d, *J* = 8.52Hz, 1H), 7.73 (t, *J* = 7.88Hz, 1H), 7.14 (t, *J* = 7.86Hz, 1H), 2.59 (dd, *J* = 18.64, 2.64Hz, 1H), 2.51 (d, *J* = 13.84Hz, 1H), 2.12–2.01 (m, 2H), 1.85–1.58 (m, 9H), 1.44–1.38 (m, 3H), 1.35 (s, 3H), 1.32–1.12 (m, 4H), 0.98 (s, 3H), 0.52 (s, 3H); ^{13}C NMR (100MHz, $CDCl_3$, ppm): δ 222.19, 166.71, 158.06, 136.80, 135.15, 134.49, 126.18, 121.81, 119.85, 56.96, 54.69, 54.23, 48.66, 48.47, 41.05, 39.43, 39.31, 38.21, 37.84, 37.55, 37.15, 30.00, 21.53, 20.13, 19.81, 18.49, 13.03; HRMS (ESI, *m/z*) calcd for $C_{27}H_{35}N_4O_4$ $[M+H]^+$ 479.2658. Found: 479.2655.

4.2.4.18. Compound ***5r***. Pale yellow solid. Yield 41%; Mp 117.3–118.5 °C; IR (KBr): 3270, 3099, 2935, 2851, 1735, 1615, 1560, 1531, 1454, 1352, 1251, 1173, 1092, 1052, 977, 939, 886, 799, 737cm^{-1}; ^1H NMR (400MHz, $CDCl_3$, ppm): δ 10.18 (s, 1H), 8.40 (s, 1H), 7.90 (d, *J* = 8.04Hz, 1H), 7.79 (dd, *J* = 8.08, 1.64Hz, 1H), 7.52 (t, *J* = 8.16Hz, 1H), 2.60–2.54 (m, 2H), 2.14–2.11 (m, 2H), 1.86–1.57 (m, 9H), 1.46–1.39 (m, 3H), 1.37 (s, 3H), 1.28–1.02 (m, 4H), 0.98 (s, 3H), 0.54 (s, 3H); ^{13}C NMR (100MHz, $CDCl_3$, ppm): δ 222.77, 166.23, 159.60, 148.99, 139.52, 130.32, 123.39, 117.19, 110.97, 57.06, 54.63, 54.13, 48.77, 48.40, 41.16, 39.54, 39.45, 38.22, 37.89, 37.71, 37.18, 30.00, 21.74, 20.18, 19.82, 18.45, 13.03; HRMS (ESI, *m/z*) calcd for $C_{27}H_{35}N_4O_4$ $[M+H]^+$ 479.2658. Found: 479.2656.

4.2.4.19. Compound ***5s***. Pale yellow solid. Yield 79%; Mp 128.3–128.9 °C; IR (KBr): 3270, 3104, 2936, 2851, 1734, 1625, 1592, 1554, 1514, 1453, 1334, 1260, 1177, 1111, 1052, 975, 851, 750, 691cm^{-1}; ^1H NMR (400MHz, $CDCl_3$, ppm): δ 9.67 (s, 1H), 8.25 (d, *J* = 9.08Hz, 2H), 7.62 (d, *J* = 9.08Hz, 2H), 2.57 (dd, *J* = 18.64, 3.20Hz, 1H), 2.52 (d, *J* = 13.92Hz, 1H), 2.12–2.01 (m, 2H), 1.79–1.56 (m, 9H), 1.46–1.37 (m,

3H), 1.35 (s, 3H), 1.27–1.01 (m, 4H), 0.98 (s, 3H), 0.52 (s, 3H); ^{13}C NMR (100MHz, $CDCl_3$, ppm): δ 222.70, 166.39, 158.89, 143.94, 142.30, 125.67, 125.67, 116.57, 116.57, 56.99, 54.55, 54.14, 48.80, 48.45, 41.16, 39.43, 39.37, 38.18, 37.84, 37.63, 37.14, 29.99, 21.44, 20.16, 19.81, 18.43, 13.08; HRMS (ESI, *m/z*) calcd for $C_{27}H_{35}N_4O_4$ $[M+H]^+$ 479.2658. Found: 479.2655.

4.2.4.20. Compound ***5t***. White solid. Yield 61%; Mp 96.0–97.8 °C; IR (KBr): 3281, 3097, 2933, 2849, 1736, 1619, 1556, 1531, 1474, 1455, 1396, 1315, 1131, 1102, 1048, 976, 866, 822, 767, 696cm^{-1}; ^{1}H NMR (400MHz, $CDCl_3$, ppm): δ 8.34 (d, J = 8.88Hz, 1H), 7.41 (s, 1H), 7.29 (d, J = 9.34Hz, 1H), 2.60 (dd, J = 18.64, 2.96Hz, 1H), 2.49 (d, J = 13.24Hz, 1H), 2.17–1.99 (m, 2H), 1.83–1.56 (m, 10H), 1.44–1.36 (m, 3H), 1.32 (s, 3H), 1.25–1.13 (m, 3H), 0.97 (s, 3H), 0.53 (s, 3H); ^{13}C NMR (100MHz, $CDCl_3$, ppm): δ 222.17, 166.14, 158.47, 133.17, 128.83, 128.25, 127.57, 121.33, 119.08, 56.96, 54.68, 54.25, 48.70, 48.49, 41.15, 39.48, 39.33, 38.26, 37.85, 37.54, 37.15, 30.03, 21.54, 20.15, 19.83, 18.49, 13.09; HRMS (ESI, *m/z*) calcd for $C_{27}H_{34}Cl_2N_3O_2$ $[M+H]^+$ 502.2028. Found: 502.2024.

4.2.4.21. Compound ***5u***. White solid. Yield 42%; Mp 248.6–250.3 °C; IR (KBr): 3176, 3062, 2941, 2847, 1738, 1629, 1563, 1450, 1375, 1255, 1214, 1110, 1028, 976, 769, 694, 591cm^{-1}; ^{1}H NMR (400MHz, $CDCl_3$, ppm): δ 7.10 (s, 3H), 2.42–2.37 (m, 2H), 2.26 (s, 6H), 1.99–1.89 (m, 1H), 1.69–1.34 (m, 11H), 1.30–1.23 (m, 2H), 1.21 (s, 3H), 1.17–1.14 (m, 4H), 0.95 (s, 3H), 0.38 (s, 3H); ^{13}C NMR (100MHz, $CDCl_3$, ppm): δ 222.48, 165.29, 162.35, 136.03, 136.03, 134.98, 128.40, 128.40, 127.37, 57.11, 54.55, 54.20, 48.67, 48.28, 41.19, 39.60, 39.27, 37.86, 37.71, 37.29, 37.17, 29.57, 20.79, 20.11, 19.83, 18.38, 18.24, 18.23, 12.56; HRMS (ESI, *m/z*) calcd for $C_{29}H_{40}N_3O_2$ $[M+H]^+$ 462.3121. Found: 462.3116.

4.2.5. Compound 6

Phenyl isocyanate (0.131 g, 1.1 mmol) was added to a solution of compound **3** (0.332 g, 1 mmol) in CH_2Cl_2 at room temperature. After stirring for 1h, the solvent was removed under vacuo. The mixture was extracted with $CH_3CO_2C_2H_5$ and H_2O, and the organic layer washed with saturated NaCl aqueous solution, dried with anhydrous sodium sulfate, filtered and concentrated under vacuum. The residue was purified by column chromatography on silica (petroleum ether/ethyl acetate = 5:1, v/v) to give the compound **6** as a white powder. Yield 96%; Mp 118.6–120.3 °C; IR (KBr): 3266, 3062, 2929, 2848, 1738, 1635, 1509, 1468, 1373, 1314, 1242, 1087, 1110, 1045, 976, 929, 899, 861, 799, 711, 588, 508, 449cm^{-1}; ^{1}H NMR (400MHz, $CDCl_3$, ppm): δ 10.19 (s, 1H), 8.79 (s, 1H), 7.84 (d, J = 7.28Hz, 2H), 7.49 (t, J = 7.42Hz, 1H), 7.36 (t, J = 7.70Hz, 2H), 2.59 (dd, J = 18.60, 3.64Hz, 1H), 2.16 (d, J = 14.56Hz, 1H), 1.97–1.78 (m, 3H), 1.74–1.59 (m, 5H), 1.55–1.34 (m, 5H), 1.24 (s, 3H), 1.20–1.11 (m, 4H), 0.97 (s, 3H), 0.92–0.88 (m, 1H), 0.78 (s, 3H);

^{13}C NMR (100MHz, $CDCl_3$, ppm): δ 222.43, 174.43, 164.45, 132.20, 131.17, 128.51, 128.51, 127.33, 127.33, 57.71, 54.64, 54.16, 48.69, 48.33, 43.36, 41.57, 39.94, 39.42, 38.08, 37.28, 37.22, 30.00, 21.96, 20.29, 19.84, 19.12, 13.65; HRMS (ESI, *m/z*) calcd for $C_{27}H_{38}N_3O_3$ $[M+H]^+$ 452.2913. Found: 452.2916.

4.2.6. Compound 7

$NaBH_4$ (0.244 g, 2 mmol) was added to a solution of compound **5a** (0.433 g, 1 mmol) in EtOH at room temperature for 3h. After completion the solvent was removed in vacuo. The residue was diluted with saturated NaCl aqueous solution and extracted with $CH_3CO_2C_2H_5$. The combined organic layer was dried over anhydrous sodium sulfate, filtered and concentrated. The residue was purified by column chromatography on silica (petroleum ether/ethyl acetate = 2:1, v/v) to give the compound **7** as a white solid. Yield 98%; Mp 129.5–130.7 °C; IR (KBr): 3253, 3139, 3055, 2935, 2844, 1720, 1628, 1599, 1560, 1499, 1451, 1373, 1321, 1246, 1171, 1147, 1118, 1052, 998, 971, 897, 749, 692, 632, 570, 502cm^{-1}; ^{1}H NMR (400MHz, $CDCl_3$, ppm): δ 7.87 (s, 1H), 7.45 (d, J = 8.52Hz, 2H), 7.33 (t, J = 7.98Hz, 2H), 7.03 (t, J = 7.36Hz, 1H), 3.85 (dd, J = 10.56, 4.64Hz, 1H), 2.49 (d, J = 13.48Hz, 1H), 2.13–2.06 (m, 1H), 1.89 (d, J = 12.40Hz, 1H), 1.78–1.66 (m, 4H), 1.55–1.32 (m, 8H), 1.25 (s, 3H), 1.24–0.93 (m, 6H), 0.90 (s, 3H), 0.55 (s, 3H); ^{13}C NMR (100MHz, $CDCl_3$, ppm): δ 165.79, 159.69, 138.10, 129.30, 129.30, 122.65, 117.27, 117.27, 80.51, 57.10, 55.76, 55.19, 42.87, 42.01, 41.97, 41.49, 39.68, 38.29, 37.88, 37.48, 33.58, 30.01, 24.86, 21.51, 20.27, 18.47, 12.93; HRMS (ESI, *m/z*) calcd for $C_{27}H_{38}N_3O_2$ $[M+H]^+$ 436.2964. Found: 436.2960.

4.2.7. Compound 8

A mixture of compound **7** (0.435 g, 1 mmol) and acetic anhydride (0.306 g, 3 mmol) in pyridine was stirred at room temperature with stirring until completion of the reaction as monitored by TLC and then concentrated under reduced pressure. Saturated NaCl aqueous solution was added and extracted with CH_2Cl_2. The organic layer was dried over anhydrous sodium sulfate, filtered and concentrated. The crude product was purified by column chromatography on silica (petroleum ether / ethyl acetate = 5:1, v/v) to afford the pure product **8** as a white solid. Yield 97%; Mp 245.2–247.1 °C; IR (KBr): 3255, 3060, 2942, 2848, 1735, 1633, 1602, 1566, 1501, 1453, 1370, 1248, 1173, 1146, 1118, 1060, 1034, 974, 749, 690, 635cm^{-1}; ^{1}H NMR (400MHz, $CDCl_3$, ppm): δ 8.00 (s, 1H), 7.47 (d, J = 7.72Hz, 2H), 7.33 (t, J = 7.98Hz, 2H), 7.04 (t, J = 7.36Hz, 1H), 4.69 (dd, J = 10.36, 4.60Hz, 1H), 2.51 (d, J = 13.40Hz, 1H), 2.12–2.08 (m, 1H), 2.02 (s, 3H), 1.90–1.72 (m, 5H), 1.62–1.32 (m, 8H), 1.28 (s, 3H), 1.25–1.20 (m, 2H), 1.08–0.92 (m, 3H), 0.90 (s, 3H), 0.52 (s, 3H); ^{13}C NMR (100MHz, $CDCl_3$, ppm): δ 171.60, 165.71, 159.75, 138.15,

129.30, 129.30, 122.62, 117.23, 117.23, 81.67, 57.11, 55.55, 54.68, 42.23, 41.42, 41.28, 40.77, 39.72, 38.25, 37.90, 37.47, 34.43, 29.87, 24.88, 21.48, 21.21, 20.06, 18.41, 12.96; HRMS (ESI, *m/z*) calcd for $C_{29}H_{40}N_3O_3$ $[M+H]^+$ 478.3070. Found: 478.3067.

4.3. General procedure for cytotoxicity assay

Cytotoxicity assay *in vitro*: HCT-116, HGC-27 and JEKO-1 cells were cultured in RPMI-1640 medium (GIBCO：31800-022) supplemented with 10% FBS, 100 U/mL of penicillin and 100 mg/mL of streptomycin at 37 ^oC in a 5% CO_2 humidified atmosphere. Cell cytotoxicity was assayed by MTT method. Briefly, cells were seeded in 96-well tissue culture plates. After 24 h incubation at 37 ^oC, 5% CO_2, removed the culture medium and replaced with fresh medium containing the studied compounds in different concentrations to the wells, and the cells were incubated for another 72 h. Afterwards, the MTT (MP: 102227) solution (0.5 mg/mL) was added and incubated for an additional 4 h. Two hundred microliters of DMSO was added to each well to dissolve the reduced MTT crystals. Optical density of each well was measured at 492/630 nm with enzyme immunoassay instrument (TECAN: Infinite 200 Pro). Then the inhibitory percentage of each compound at various concentrations to the cell proliferation was calculated, and the IC_{50} value was determined.

4.4. Computational studies

The computational studies containing 2D-HQSAR and 3D-Topomer CoMFA were carried out by using the SYBYL (Tripos Inc., St. Louis, USA) following the standard procedures provided in the manual. 2D-HQSAR was run from SYBYL using default parameters: hologram lengths (53, 59, 61, 71, 83, 97, 151, 199, 257, 307, 353 and 401), atom count in fragments (min = 4 and max = 7) were used. The best model was selected on the basis of best crossvalideted r^2. Two options dialog boxes, which are show statistics for model ensemble and retain fragment information for prediticton statistics, were checked. For the 3D-topomer CoMFA, all the training set compounds were automatically divided into R_1 and R_2 fragments and followed by automated PLS analysis, fragment alignment and activity predictions. Statistical parameters such as q^2, r^2, number of components were generated. Standard errors of prediction were recorded for both sets and steric and electrostatic contour maps were obtained.

Acknowledgments

We look forward to financial support from the National Natural Science Foundation of China (Project No. 20772113), Scientific Research Fund of Xinxiang Medical University (2014QN148) and the Doctoral Foundation of Henan Institute of Engineering (D09002).

Supplementary data

Supporting information file related to this article is named as Appendix S1 which can be found at XXX

References and notes

1. Siegel R.L., Miller K.D., Jemal A. (2016) Cancer statistics, 2016. Cancer J Clin;66:7-30.
2. Ferlay J., Soerjomataram I., Dikshit R., Eser S., Mathers C., Rebelo M., Parkin D.M., Forman D., Bray F. (2015) Cancer incidence and mortality worldwide: sources, methods and major patterns in GLOBOCAN 2012. Int J Cancer;136:E359-E386.
3. Seguin L., Desgrosellier J.S., Weis S.M., Cheresh D.A. (2015) Integrins and cancer: regulators of cancer stemness, metastasis, and drug resistance. Trends cell Biol;25:234-240.
4. Beghyn T., Deprez-Poulain R., Willand N., Folleas B., Deprez B. (2008) Natural compounds: leads or ideas? Bioinspired molecules for drug discovery. Chem Biol Drug Des;72:3-15.
5. Chen J.W., Wu Q.H., Rowley D.C., Al-Kareef A.M., Wang H. (2015) Anticancer agent-based marine natural products and related compounds. J Asian Nat Prod Res;17:199-216.
6. John J.E. (2009) Natural products-based drugs and membrane permeability, a hypothesis. Chem Biol Drug Des;73:367-368.
7. Pan L., Chai H., Kinghorn A.D. (2010) The continuing search for antitumor agents from higher plants. Phytochem Lett;3:1-8.
8. Cragg G.M., Newman D.J., Snader K.M. (1997) Natural products in drug discovery and development. J Nat Prod;60:52-60.
9. Mosettig E., Beglinger U., Dolder F., Lichti H., Quitt P., Waters, J.A. (1963) The absolute configuration of steviol and isosteviol. J Am Chem Soc;85:2305-2309.
10. Avent A.G., Hanson J.R., De Oliveira B.H. (1990) Hydrolysis of the diterpenoid glycoside, stevioside. Phytochemistry;29:2712-2715.
11. Liu J.C., Kao P.F., Hsieh M.H., Chen Y.J., Chan P. (2001) The antihypertensive effect of stevioside derivative isosteviol in spontaneously hypertensive rats. Acta Cardiol Sin;17:133-140.
12. Wong K.L., Chan P., Yang H.Y., Hsu F.L., Liu I.M., Cheng Y.W., Cheng J.T. (2004) Isosteviol acts on potassium channels to relax isolated aortic strips of Wistar rat. Life Sci;74:2379-2387.
13. Yamamoto N.S., Bracht A.M.K., Ishii E.L., Kemmelmeier F. S., Alvarez M., Bracht A. (1985) Effect of steviol and its structural analogues on glucose production and oxygen uptake in rat renal tubules. Experientia;41:55-57.
14. Ma J., Ma Z., Wang J., Milne R.W., Xu D., Davey A.K., Evans A.M. (2007) Isosteviol reduces plasma glucose levels in the intravenous glucose tolerance test in Zucker diabetic fatty rats. Diabetes Obes Metab;9:597-599.
15. Wong K.L., Wu K.C., So E.C., Wu R.S.C., Cheng T.H. (2007) The anti-oxidative effect of isosteviol on angiotensin-II-induced reactive oxygen species generation in hypertensive injury of aortic smooth muscle cells: 9AP8-1. Eur J Anaesth;24:125.
16. Chatsudthipong V, Muanprasat C. (2009) Stevioside and related compounds: therapeutic benefits beyond sweetness. Pharmacol Therapeut;121:41-54.
17. Xu D., Li Y., Wang J., Davey A.K., Zhang S., Evans A.M. (2007) The cardioprotective effect of isosteviol on rats with heart ischemia-reperfusion injury. Life Sci;80:269-274.
18. Xu D., Du W., Zhao L., Davey A.K., Wang J. (2008) The neuroprotective effects of isosteviol against focal cerebral ischemia injury induced by middle cerebral artery occlusion in rats. Planta Med;74:816-821.

19. Takasaki M., Konoshima T., Kozuka M., Tokuda H., Takayasu J., Nishino H., Miyakoshi M., Mizutani K., Lee K.H. (2009) Cancer preventive agents. Part 8: Chemopreventive effects of stevioside and related compounds. Bioorgan Med Chem;17: 600-605.
20. Lohoelter C., Weckbecker M., Waldvogel S.R. (2013) (–)-Isosteviol as a versatile ex-chiral-pool building block for organic chemistry. Eur J Org Chem;2013:5539-5554.
21. Wang T.T., Liu Y., Chen L. (2014) Synthesis and cytotoxic activity of nitric oxide-releasing isosteviol derivatives. Bioorgan Med Chem Lett;24:2202-2205.
22. Khaybullin R.N., Liang X., Cisneros K., Qi X. (2015) Synthesis and anticancer evaluation of complex unsaturated isosteviol-derived triazole conjugates. Future Med Chem;7:2419-2428.
23. Liu C.J., Yu S.L., Liu Y.P., Dai X.J., Wu Y., Li R.J., Tao J.C. (2016) Synthesis, cytotoxic activity evaluation and HQSAR study of novel isosteviol derivatives as potential anticancer agents. Eur J Med Chem;115:26-40.
24. An Y.J., Zhang Y.X., Wu Y., Liu Z.M., Pi C., Tao J.C. (2010) Simple amphiphilic isosteviol–proline conjugates as chiral catalysts for the direct asymmetric aldol reaction in the presence of water. Tetrahedron: Asymmetry;21:688-694.
25. Ma Z.W., Liu Y.X., Zhang W.J., Tao Y., Zhu Y., Tao J.C., Tang M.S. (2011) Highly Enantioselective Michael Additions of Isobutyraldehyde to Nitroalkenes Promoted by Amphiphilic Bifunctional Primary Amine-Thioureas in Organic or Aqueous Medium. Eur J Org Chem;2011:6747-6754.
26. Geng Z.C., Chen X., Zhang J.X., Li N., Chen J., Huang X.F., Wang X.W. (2013) Asymmetric Michael/Aromatization Reaction of Azlactones to α, β-Unsaturated Pyrazolones with C-4 Regioselectivity Catalyzed by an Isosteviol-Derived Thiourea Organocatalyst. Eur J Org Chem;2013: 4738-4743.
27. Song Z.T., Zhang T., Du H.L., Ma Z.W., Zhang C.H., Tao J.C. (2014) Highly Enantioselective Michael Addition Promoted by a New Diterpene-Derived Bifunctional Thiourea Catalyst: A Doubly Stereocontrolled Approach to Chiral Succinimide Derivatives. Chirality;26:121-127.
28. Zhang T., Wu Y., Gao L.H., Song Z.T., Zhao L., Zhang Y.X., Tao, J.C. (2013) A novel Na+ coordination mediated supramolecular organogel based on isosteviol: water-assisted self-assembly, in situ forming and selective gelation abilities. Soft Matter;9:638-642.
29. Voronin M.A., Gabdrakhmanov D.R., Khaibullin R.N., Strobykina I.Y., Kataev V.E., Idiyatullin B.Z., Konovalov A.I. (2013) Novel biomimetic systems based on amphiphilic compounds with a diterpenoid fragment: Role of counterions in self-assembly. J Colloid Interf Sci;405:125-133.
30. Gabdrakhmanov D.R., Voronin M.A., Zakharova L.Y., Konovalov A.I., Khaybullin R.N., Strobykina I.Y., Salnikov V.V. . (2013) Supramolecular design of biocompatible nanocontainers based on amphiphilic derivatives of a natural compound isosteviol. Phys Chem Chem Phys;15:16725-16735.
31. Li J, Zhang D, Wu X. (2011) Synthesis and biological evaluation of novel exo-methylene cyclopentanone tetracyclic diterpenoids as antitumor agents. Bioorgan Med Chem Lett;21:130-132.
32. Zhang T., Lu L.H., Liu H., Wang J.W., Wang R.X., Zhang Y.X., Tao J.C. (2012) D-ring modified novel isosteviol derivatives: Design, synthesis and cytotoxic activity evaluation. Bioorgan Med Chem Lett;22:5827-5832.
33. Khaybullin R.N., Zhang M., Fu J., Liang X., Li T., Katritzky A.R., Okunieff P., Qi X. (2014) Design and synthesis of isosteviol triazole conjugates for cancer therapy. Molecules;19:18676-18689.
34. Zhu S.L., Wu Y., Liu C.J., Wei C.Y., Tao J.C., Liu H.M. (2013) Synthesis and in vitro cytotoxic activity evaluation of novel heterocycle bridged carbothioamide type isosteviol derivatives as antitumor agents. Bioorgan Med Chem Lett;23:1343-1346.

35. Zhang C., Du C., Feng Z., Zhu J., Li Y. (2015) Hologram quantitative structure activity relationship, docking, and molecular dynamics studies of inhibitors for CXCR4. Chem Biol Drug Des;85:119-136.
36. Wu Y., Yang J.H., Dai G.F., Liu C.J., Tian G.Q., Ma W.Y., Tao J.C. (2009) Stereoselective synthesis of bioactive isosteviol derivatives as α-glucosidase inhibitors. Bioorgan Med Chem;17:1464-1473.

Figure legends

Synthesis, cytotoxic activity, 2D- and 3D-QSAR studies of 19-carboxyl modified novel isosteviol derivatives as potential anticancer agents

Cong-Jun Liu [a], Tao Zhang [b], Shu-Ling Yu [c], Xing-Jie Dai [a], Ya Wu [a], Jing-Chao Tao* [a]

[a] College of Chemistry and Molecular Engineering, New Drug Research & Development Center, Zhengzhou University, 75 Daxue Road, Zhengzhou, Henan 450052, China

[b] School of Pharmacy, Xinxiang Medical University, Xinxiang 453003, Henan, China

[c] Key Laboratory of Natural Medicine and Immune-Engineering of Henan Province, Henan University, Kaifeng, Henan 475004, China

Fig. 1. Chemical structures of compounds **A**-**E**

Fig. 2. Fragmentation pattern (R_1 and R_2) for all molecules of dataset in 3D-topomer CoMFA analysis

Fig. 3. The histogram of residuals between experimental values versus predicted values of pIC_{50} of the test set in the 2D-HQSAR and 3D-topomer CoMFA model

Fig. 4. Scatter plots of experimental values versus predicted values of pIC_{50} of the training and test set from 2D-HQSAR (**A**) and 3D-topomer CoMFA (**B**) analyses, respectively.

Fig. 5. The 2D-HQSAR contribution maps of compounds **4s**, **4u**, **5f** and **5t**

Fig. 6. Contour maps of 3D-topomer CoMFA. (**A**) Steric contour map depicted around R_1; (**B**) electrostatic contour map depicted around R_1; (**C**) Steric contour map depicted around R_2; (**D**) electrostatic contour map depicted around R_2.

Scheme 1. *Reagents and conditions:* (i) oxalyl chloride, DMF, DCM, rt, 8h; (ii) $N_2H_4 \cdot H_2O$, DCM, -10 ^oC, 1 h, 89%; (iii) isothiocyanates, DCM, rt, 0.5h; (iv) $Hg(OAc)_2$, EtOH, reflux, 5h.

Scheme 2. *Reagents and conditions:* (i) phenyl isocyanate, DCM, rt, 1h, 96%; (ii) $NaBH_4$, EtOH, rt, 3h, 98%; (iii) Ac_2O, pyridine, rt, 6h, 97%.

Tables:

Synthesis, cytotoxic activity, 2D- and 3D-QSAR studies of 19-carboxyl modified novel isosteviol derivatives as potential anticancer agents

Cong-Jun Liu [a], Tao Zhang [b], Shu-Ling Yu [c], Xing-Jie Dai [a], Ya Wu [a], Jing-Chao Tao* [a]

[a] College of Chemistry and Molecular Engineering, New Drug Research & Development Center, Zhengzhou University, 75 Daxue Road, Zhengzhou, Henan 450052, China

[b] School of Pharmacy, Xinxiang Medical University, Xinxiang 453003, Henan, China

[c] Key Laboratory of Natural Medicine and Immune-Engineering of Henan Province, Henan University, Kaifeng, Henan 475004, China

Table 1. Cytotoxic activities of isosteviol derivatives *in vitro* from different cancer types [a]

Cd	Cytotoxic activities (IC_{50}, μM)[b,c]			Cd	Cytotoxic activities (IC_{50}, μM)[b,c]		
	HCT-11	HGC-27	JEKO-1		HCT-11	HGC-27	JEKO-1
1	>100	>100	>100	5b	8.56±0.4	9.87±0.4	16.51±1.1
3	15.20±0.5	27.42±0.9	5.17±0.3	5c	7.92±0.9	12.47±1.1	29.34±1.1
4a	3.43±0.2	6.72±0.7	3.66±0.3	5d	14.00±0.5	14.54±0.9	36.61±3.8
4b	11.61±0.9	12.04±0.3	10.18±0.5	5e	7.17±0.5	9.65±0.3	3.39±0.2
4c	3.75±0.4	6.15±0.6	4.21±0.1	5f	5.00±0.6	11.98±1.0	3.73±0.3
4d	3.92±0.1	6.78±0.2	9.08±0.3	5g	7.56±0.4	6.22±0.1	2.50±0.1
4e	3.69±0.3	7.19±0.9	11.62±1.1	5h	14.70±0.7	7.49±0.1	16.21±0.8
4f	1.84±0.1	3.11±0.3	3.15±0.3	5i	18.78±0.3	17.18±1.2	10.95±0.5
4g	2.40±0.5	5.33±0.9	4.85±0.1	5j	11.20±0.2	16.84±1.7	15.56±0.8
4h	5.14±0.8	11.31±0.7	21.77±1.6	5k	12.26±0.9	11.68±0.4	24.53±1.2
4i	1.62±0.1	2.89±0.3	3.36±0.3	5l	12.89±0.9	20.25±1.2	19.00±1.3
4j	2.07±0.3	4.95±0.1	7.77±0.8	5m	10.22±0.8	15.60±1.3	27.83±0.9
4k	8.26±0.4	10.78±1.1	14.76±0.7	5n	6.43±0.3	12.22±0.4	22.77±0.1
4l	1.35±0.3	2.31±0.1	3.08±0.4	5o	12.45±0.5	11.41±0.3	16.42±0.5
4m	1.60±0.1	2.94±0.1	3.20±0.2	5p	8.69±0.7	10.33±0.5	39.76±2.3
4n	8.71±0.9	9.19±0.8	25.00±2.3	5q	14.95±0.2	26.00±1.3	39.92±0.6
4o	3.62±0.6	4.91±0.8	10.45±0.6	5r	10.14±0.3	14.67±1.1	31.89±0.8
4p	6.25±0.6	7.24±0.6	14.08±0.1	5s	6.40±0.1	8.54±0.1	31.72±1.3
4q	9.36±0.4	24.33±0.4	31.86±2.7	5t	32.91±1.6	18.22±0.5	76.52±3.6
4r	1.134±0.1	2.77±0.1	2.57±0.1	5u	27.17±0.9	16.73±0.5	91.80±13.2
4s	0.95±0.1	2.65±0.2	2.96±0.3	6	16.74±1.3	12.53±0.5	23.64±0.6
4t	3.08±0.2	9.82±0.7	13.57±1.3	7	8.39±0.7	17.51±0.8	57.24±2.5

4u	13.61±0.9	17.12±1.0	27.15±1.2	8	15.06±1.3	17.50±0.8	52.53±2.4
5a	9.56±0.9	11.64±0.3	32.08±2.8	Cisplatin	3.91±0.3	2.03±0.1	2.74±0.2

[a] HTC-116 is colon-derived; HGC-27 is gastric-derived and JEKO-1 is mantle cell lymphoma-derived

[b] Values are the mean of triplicate of three independent experiments

[c] ±SD

Table 2. 2D-HQSAR analysis for various fragment distinction using default fragment size (4–7)

model	Fragment distinction	q^2	SEcv	r^2	SEE	HL	N
1	A/B	0.413	0.294	0.636	0.232	199	2
2	A/B/C	0.368	0.310	0.683	0.220	307	3
3	A/B/H	0.498	0.281	0.756	0.196	401	4
4	A/B/Ch	0.516	0.280	0.824	0.169	61	5
5	A/B/DA	0.451	0.289	0.678	0.221	401	3
6	A/B/C/H	0.480	0.286	0.750	0.198	353	4
7	A/B/H/Ch	0.522	0.274	0.733	0.205	53	4
8	A/B/C/Ch	0.382	0.322	0.897	0.131	401	6
9	A/B/H/DA	0.589	0.262	0.849	0.159	83	6
10	A/B/C/DA	0.462	0.286	0.640	0.234	401	3
11	A/B/Ch/DA	0.487	0.279	0.705	0.212	401	3
12	A/B/C/H/Ch	0.485	0.284	0.754	0.197	353	4
13	A/B/H/Ch/DA	0.577	0.262	0.837	0.163	83	5
14	A/B/C/Ch/DA	0.455	0.288	0.636	0.235	401	3
15	A/B/C/H/Ch/DA	0.539	0.278	0.849	0.159	401	6

q^2: cross-validated correlation coefficient (LOO). SE_{CV}: cross-validated standard error. r^2: noncross-validated correlation coefficient. SEE: noncross validated standard error. HL: hologram length. N: optimum number of component. Fragment distinction: A-atoms, B-bonds, C-connections, H-hydrogen, Ch-chirality, DA-donor and acceptor.

Table 3. 2D-HQSAR analysis for the influence of fragment sizes using the best fragment distinction (A/B/H/DA)

model	Fragment size	q^2	SEcv	r^2	SEE	HL	N
1	1–3	0.423	0.288	0.508	0.266	59	1
2	2–4	0.555	0.273	0.793	0.186	71	6
3	3–5	0.551	0.270	0.805	0.178	401	5
4	3–7	0.587	0.263	0.848	0.159	83	6

5	4–6	0.569	0.269	0.831	0.168	53	6
6	4–7	0.589	0.262	0.849	0.159	83	6
7	4–8	0.625	0.246	0.850	0.156	71	5
8	5–8	0.630	0.245	0.850	0.156	71	5
9	5–9	0.577	0.266	0.856	0.155	71	6
10	6–7	0.576	0.266	0.844	0.162	97	6
11	6–8	0.637	0.243	0.853	0.154	71	5
12	6–9	0.613	0.255	0.875	0.145	61	6
13	7–8	0.631	0.249	0.882	0.140	97	6
14	7–9	0.590	0.262	0.876	0.144	61	6
15	8–9	0.566	0.270	0.823	0.172	151	6

Table 4. Statistical parameters of the optimal 2D-HQSAR and 3D-topomer CoMFA models

Model method	q^2	SEcv	r^2	SEE	N	r^2_{pred}
2D-HQSAR	0.631	0.249	0.882	0.140	6	0.832
3D-topomer CoMFA	0.572	0.250	0.853	0.150	3	0.643

Table 5. Experimental and predicted activities (pIC_{50}) with residual values for the nine test set compounds investigating the predictability of 2D-HQSAR and 3D-topomer CoMFA models

Cd	Exp (pIC_{50})	2D-HQSAR model		3D-topomer CoMFA model	
		Pred (pIC_{50})	Res	Pred (pIC_{50})	Res
4a	-0.535	-0.565	0.030	-0.465	-0.070
4b	-1.065	-0.811	-0.254	-0.683	-0.382
4j	-0.316	-0.375	0.059	-0.308	-0.008
4r	-0.057	-0.344	0.288	-0.199	0.143
4u	-1.134	-1.211	0.077	-0.737	-0.397
5e	-0.856	-1.087	0.231	-1.100	0.244
5l	-1.110	-1.054	-0.056	-1.006	-0.105
5p	-0.939	-0.928	-0.011	-1.064	0.125
7	-0.924	-0.879	-0.045	-1.082	0.159

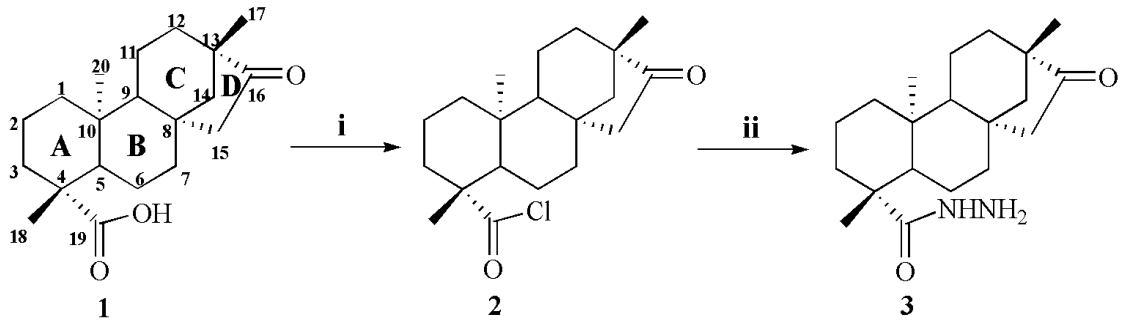

1 2 3

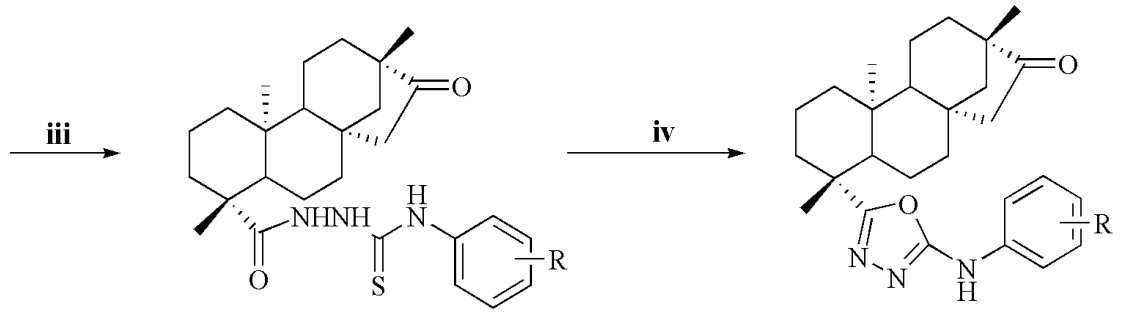

4a-4u 5a-5u

4a: R=H(64%)
4b: R=o-CH_3(60%)
4c: R=m-CH_3(37%)
4d: R=p-CH_3(41%)
4e: R=o-F(73%)
4f: R=m-F(80%)
4g: R=p-F(89%)
4h: R=o-Cl(74%)
4i: R=m-Cl(80%)
4j: R=p-Cl(88%)
4k: R=o-Br(79%)

4l: R=m-Br(67%)
4m: R=p-Br(70%)
4n: R=o-OCH_3(77%)
4o: R=m-OCH_3(89%)
4p: R=p-OCH_3(72%)
4q: R=o-NO_2(70%)
4r: R=m-NO_2(72%)
4s: R=p-NO_2(50%)
4t: R=2,4-Cl_2(75%)
4u: R=2,6-Me_2(58%)

5a: R=H(97%)
5b: R=o-CH_3(70%)
5c: R=m-CH_3(37%)
5d: R=p-CH_3(25%)
5e: R=o-F(38%)
5f: R=m-F(22%)
5g: R=p-F(58%)
5h: R=o-Cl(26%)
5i: R=m-Cl(19%)
5j: R=p-Cl(10%)
5k: R=o-Br(91%)

5l: R=m-Br(88%)
5m: R=p-Br(95%)
5n: R=o-OCH_3(44%)
5o: R=m-OCH_3(57%)
5p: R=p-OCH_3(64%)
5q: R=o-NO_2(50%)
5r: R=m-NO_2(41%)
5s: R=p-NO_2(79%)
5t: R=2,4-Cl_2(61%)
5u: R=2,6-Me_2(42%)

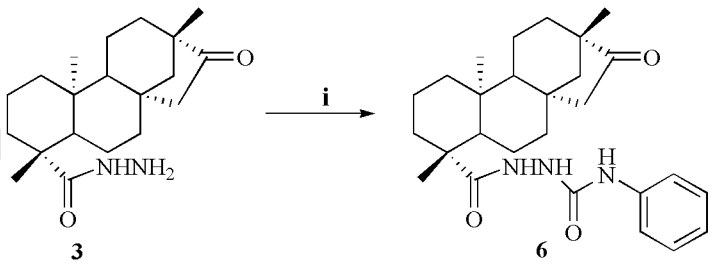

3 6

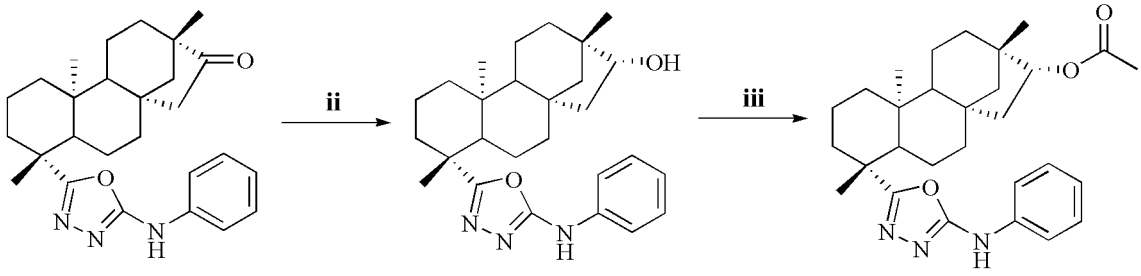

5a 7 8

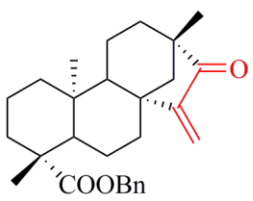

A

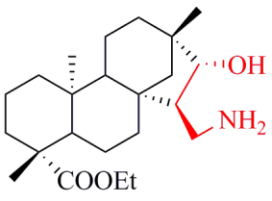

B

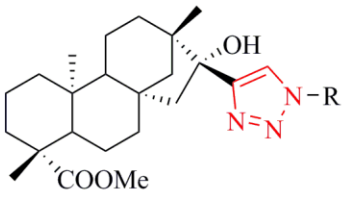

C

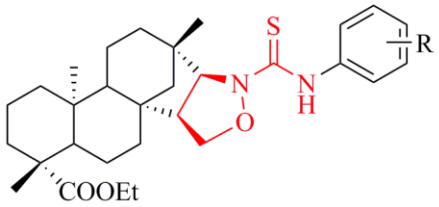

D

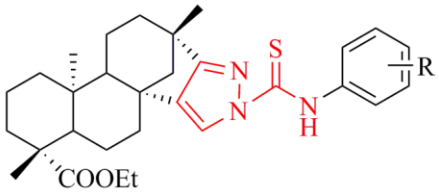

E

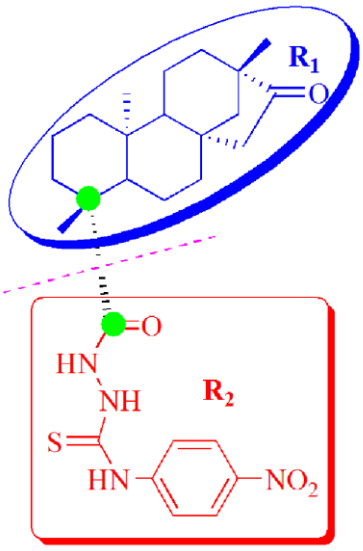

Compound **4s**

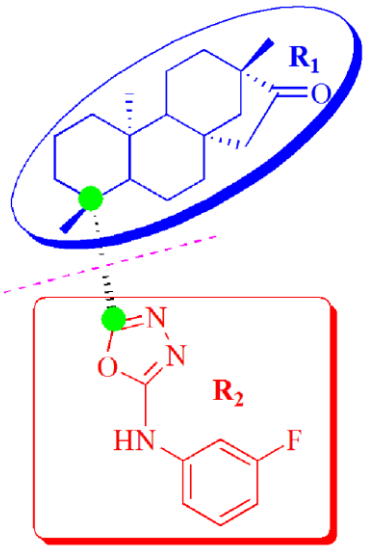

Compound **5f**

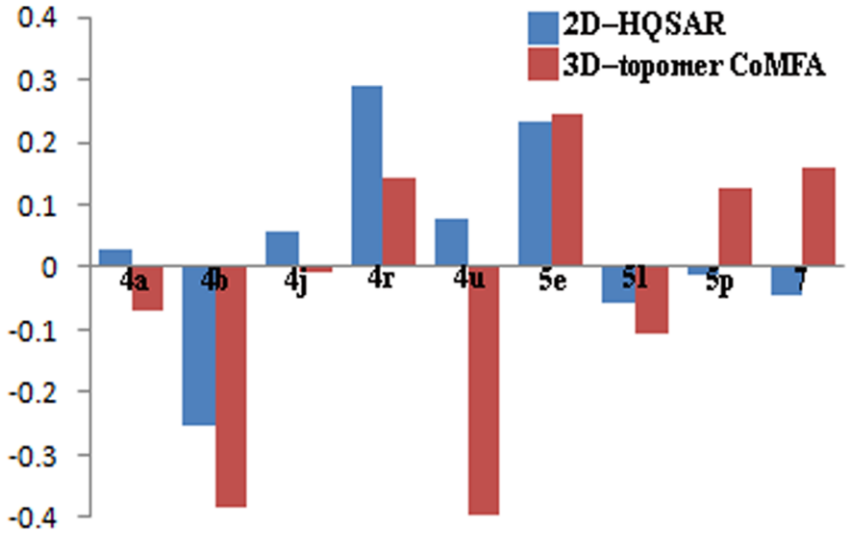

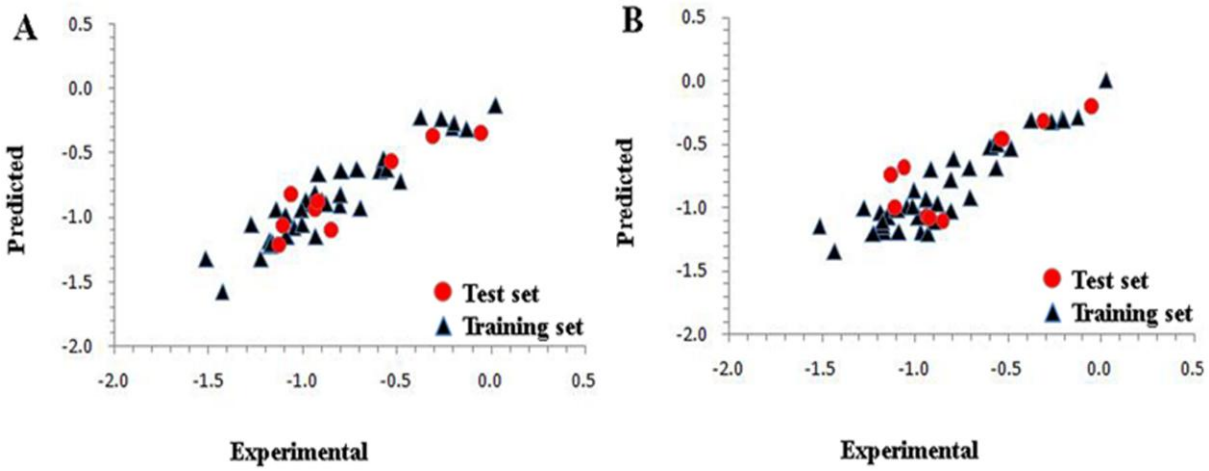

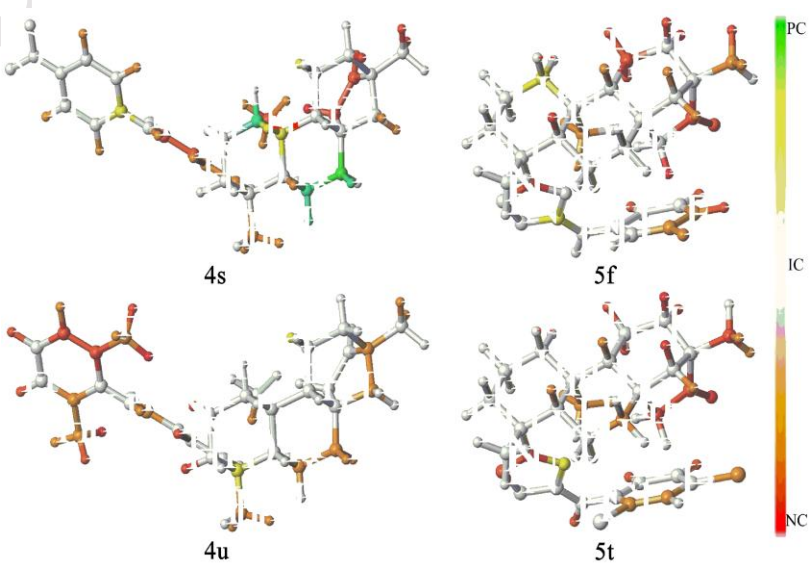

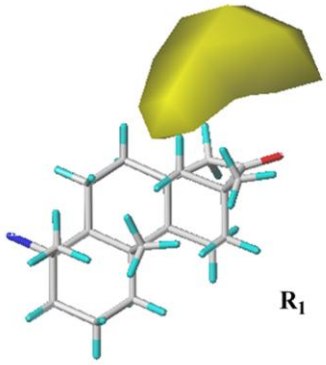

A

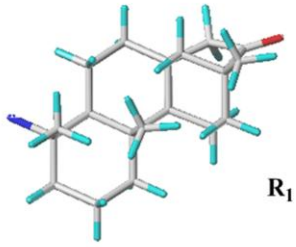

B

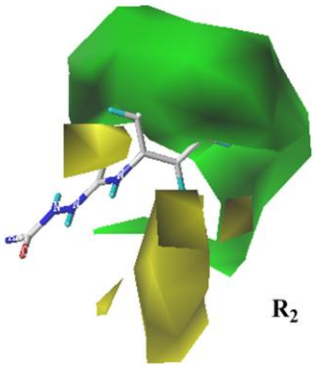

C

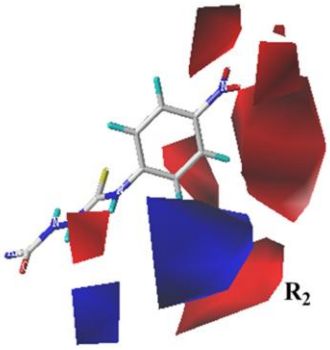

D